The Journal of Neuroscience, February 1994, 14(2): 667–696

Light and Electron Microscope Distribution of the NMDA Receptor Subunit NMDAR1 in the Rat Nervous System Using a Selective Anti-Peptide Antibody

R. S. Petralia, N. Yokotani, and R. J. Wenthold

Laboratory of Neurochemistry, NIDCD, NIH, Bethesda, Maryland 20892

NMDA receptors play key roles in synaptic plasticity and neuronal development, and may be involved in learning, memory, and compensation following injury. A polyclonal antibody that recognizes four of seven splice variants of NMDAR1 was made using a C-terminus peptide (30 amino acid residues). NMDAR1 is the major NMDA receptor subunit, found in most or all NMDA receptor complexes. On immunoblots, this antibody labeled a single major band migrating at M_r = 120,000. The antibody did not cross-react with extracts from transfected cells expressing other glutamate receptor subunits, nor did it label non-neuronal tissues. Immunostained vibratome sections of rat tissue showed labeling in many neurons in most structures in the brain, as well as in the cervical spinal cord, dorsal root and vestibular ganglia, and in pineal and pituitary glands. Staining was moderate to dense in the olfactory bulb, neocortex, striatum, some thalamic and hypothalamic nuclei, the colliculi, and many reticular, sensory, and motor neurons of the brainstem and spinal cord. The densest stained cells included the pyramidal and hilar neurons of the CA3 region of the hippocampus, Purkinje cells of the cerebellum, supraoptic and magnocellular paraventricular neurons of the hypothalamus, inferior olive, red nucleus, lateral reticular nucleus, peripheral dorsal cochlear nucleus, and motor nuclei of the lower brainstem and spinal cord. Ultrastructural localization of immunostaining was examined in the hippocampus, cerebral cortex, and cerebellar cortex. The major staining was in postsynaptic densities apposed by unstained presynaptic terminals with round or mainly round vesicles, and in associated dendrites. The pattern of staining matched that of previous *in situ* hybridization but differed somewhat from that of binding studies, implying that multiple types of NMDA receptors exist. Comparison with previous studies of localization of other glutamate receptor types revealed that NMDAR1 may colocalize with these other types in many neurons throughout the nervous system.

[Key words: excitatory amino acids, ultrastructure, immunocytochemistry, AMPA, hippocampus, cerebellum]

Glutamate and related molecules are the major excitatory neurotransmitters of the CNS (review by Monaghan et al., 1989) and their receptors play roles not only in general transmission of impulses, but also in synaptic plasticity, which forms the basis for learning, memory, neural ontogeny, and compensation from injury to the nervous system (e.g., reviews by Collingridge and Singer, 1990; Anwyl, 1991). Glutamate (or excitatory amino acid) receptors can be divided into metabotropic and ionotropic types. Ionotropic glutamate receptors can be divided further into NMDA and non-NMDA types. Numerous subunits and variants of each of these types have now been cloned and sequenced, mainly from rats, but also from mice and humans (Puckett et al., 1991; Yamazaki et al., 1992b; reviews by Nakanishi, 1992; Sommer and Seeburg, 1992). Non-NMDA, ionotropic glutamate receptors include those that bind AMPA (α-amino-3-hydroxy-5-methyl-4-isoxazolepropionate) with high affinity, that is, the AMPA receptor subunits, GluR1–GluR4 (also called GluRA–GluRD, and including flip and flop variants and GluR4c; e.g., Hollmann et al., 1989; Boulter et al., 1990; Keinänen et al., 1990; Gallo et al., 1992; review by Sommer and Seeburg, 1992). Non-NMDA, ionotropic receptors also include a second group that is more kainate selective, that is, kainate receptors, including GluR5–GluR7 and KA1 and -2 (e.g., Bettler et al., 1990; Werner et al., 1991; review by Sommer and Seeburg, 1992). Both AMPA and kainate receptors evoke fast, voltage-independent synaptic responses and thus form the basic receptors for excitatory amino acid neurotransmission (reviews by Nakanishi, 1992; Sommer and Seeburg, 1992). In addition, they play associative roles in synaptic plasticity (review by Anwyl, 1991). Some forms of these receptors, particularly those known to pass calcium through the ion channel, may be involved in specialized functions during development and in certain specialized cell types in adults (reviews by Nakanishi, 1992; Sommer and Seeburg, 1992).

While non-NMDA, ionotropic receptors form the major glutamate receptor types, it is the metabotropic and NMDA receptors that appear to be the major regulators of synaptic plasticity and other long-term changes in neurons. Cloned and sequenced metabotropic glutamate receptor subunits include mGluR1α,β,c and mGluR2–mGluR6 (e.g., Houamed et al., 1991; Masu et al., 1991; Pin et al., 1992; review by Nakanishi, 1992). Metabotropic glutamate receptors are linked to G-proteins and thus may exert long-lasting actions in neurons. They are implicated in different forms of long-term potentiation, long-term depression, and suppression of neurotransmission (Zheng and Gallagher, 1992; Kato, 1993; reviews by Anwyl, 1991; Nakanishi, 1992). NMDA receptors are perhaps the most widely

Received May 25, 1993; revised July 13, 1993; accepted July 22, 1993.

We thank Dr. Y. Wang for assistance in preparation of the manuscript; N. Alvanzo for technical help; Dr. E. Mugnaini for helping us interpret data on the cerebellar localization of NMDAR1; Drs. C. Hunter, M. Schneider, and M. Tachibana for critically reading the manuscript; and Drs. S. Heinemann, S. Nakanishi, and P. Seeburg for supplying cDNA clones.

Correspondence should be addressed to Ronald S. Petralia, Laboratory of Neurochemistry, Building 36, Room 5D-08, NIDCD, NIH, Bethesda, MD 20892.

studied glutamate receptors because of their involvement in long-term potentiation, which may underlie learning and memory (reviews by Izquierdo, 1991; Malenka, 1991), as well as their influence on neuronal development (Cline and Constantine-Paton, 1989; Fields et al., 1991; Komuro and Rakic, 1993). The general model for long-term potentiation, based mainly on studies of the CA1 hippocampal pyramidal cell (reviews by Anwyl, 1991; Malenka, 1991), involves an initial activation of postsynaptic AMPA receptors by glutamate released from the presynaptic terminal. The resulting postsynaptic depolarization removes the voltage-dependent magnesium block of the NMDA receptor channel, permitting calcium entry when the NMDA receptor is activated by glutamate released from the presynaptic terminal (Malenka, 1991). Entry of calcium into the postsynaptic cell initiates a series of events (e.g., nitric oxide release; Izumi et al., 1992) leading to long-term potentiation of postsynaptic responsiveness. In addition to their involvement in neural plasticity, NMDA receptors may be involved in normal information processing (Armstrong-James et al., 1993; review by Daw et al., 1993). NMDA receptors include two main classes of subunits, NMDAR1 and NMDAR2 (review by Nakanishi, 1992), also referred to as NR1 and NR2 (Monyer et al., 1992), as well as one type whose relationship to definitive NMDA receptors is unclear (Kumar et al., 1991). NMDAR1 (Moriyoshi et al., 1991) includes seven splice variants (R1A–R1G) generated from alternative splicing of mRNA as well as a truncated form (N. Nakanishi et al., 1992; Sugihara et al., 1992), while NMDAR2 has four subunits (Monyer et al., 1992; Nakanishi, 1992). Some similar subunits, corresponding to NMDAR1 and -2, have been described for the mouse (Ikeda et al., 1992; Kutsuwada et al., 1992; Meguro et al., 1992; Yamazaki et al., 1992a) and human (Karp et al., 1993).

NMDA receptor complexes are made up of various combinations of subunits, resulting in a variety of NMDA receptor forms with differing pharmacological and/or electrophysiological properties (review by Nakanishi, 1992). However, all NMDA receptor complexes likely contain at least one NMDAR1 subunit, which serves as the fundamental subunit required to make a functional NMDA receptor (review by Nakanishi, 1992). Consequently, it is not surprising that NMDAR1 is widespread throughout the nervous system; *in situ* hybridization studies demonstrate that NMDAR1 is present in most neurons in all regions of the brain (Moriyoshi et al., 1991; review by Nakanishi, 1992), spinal cord (Furuyama et al., 1993), and peripheral ganglia (Shigemoto et al., 1992b). Since it is found in more cells than any of the NMDAR2 subunits, a comprehensive study of distribution of NMDAR1 may be an accurate way of determining which populations of neurons in each region of the brain express NMDA receptors and where NMDA receptors are localized within these neurons. While the former can be addressed by *in situ* hybridization histochemistry, immunocytochemistry is required to localize the NMDA receptor protein within each neuron in each region of the brain. Most importantly, immunocytochemistry could provide information on the distribution of NMDA receptors that are associated with known inputs to a neuron, and thus contribute to the understanding of the role that NMDA receptors play in various neuronal circuits. However, very little has been published on antibodies to NMDAR1 (Chazot et al., 1992; Fotuhi et al., 1992; Hennegriff et al., 1992). The present article is a comprehensive survey of the localization of an antibody to four of seven known splice variants (R1A–R1C, R1F) of NMDAR1 in the nervous system of the rat, employing both light and electron microscopy. We provide data on the distribution of NMDAR1 in many types of neurons, and compare the localization of NMDAR1 with that described previously for other glutamate receptor subunits. We discuss these data in the context of previous ligand-binding autoradiography and *in situ* hybridization studies.

Materials and Methods

Antibody production and purification. A synthetic peptide (LQNQKDTVLPRRAIEREEGQLQLCSRHRES) corresponding to the C-terminus of the rat NMDAR1 (Moriyoshi et al., 1991) was prepared commercially and determined by HPLC to be greater than 97% pure. The peptide was conjugated to bovine serum albumin (BSA) with glutaraldehyde and injected into rabbits following the protocol described for making antibodies to the AMPA receptors (Wenthold et al., 1992). The antibodies were affinity purified using the peptide attached to Activated CH Sepharose 4B (Pharmacia LKB Biotechnology, Piscataway, NJ) as described previously (Petralia and Wenthold, 1992; Wenthold et al., 1992).

Antibody characterization. The specificity of the anti-NR1 antibody was determined using immunoblots of brain tissues or transfected cell membranes. The cDNA clones for the glutamate receptors were kindly provided by the following: NMDAR1, Dr. S. Nakanishi, Kyoto Univ.; GluR1-7, Dr. S. Heinemann, The Salk Institute; KA1 and KA2, Dr. P. Seeburg, Univ. Heidelberg. Whole cDNA inserts were incorporated into the eukaryotic expression vectors pcDM8, pcDNAI, or pcDNAI-amp (Invitrogen, San Diego, CA). GluR4 DNA was produced by polymerase chain reaction amplification, as described previously (Wenthold et al., 1992). The NMDAR1 cDNA was inserted into pcDNAI plasmid using the HindIII and NotI restriction sites. cDNAs were transfected into human embryonic kidney cells (HEK-293) by the calcium phosphate–DNA coprecipitation method (Chen and Okayama, 1987) with commercially obtained reagents (Specialty Media, Inc., Lavallette, NJ). Cells were harvested 48 hr after transfection and washed with 50 mM Tris HCl, pH 7.4. The expression of glutamate receptor subunits in the transfected cells was verified using antibodies selective for the subunit in all cases except for GluR5 and KA1 (Wenthold et al., 1992, in press). For analysis of NMDAR1 expression in tissues, rats were anesthetized with carbon dioxide and decapitated. Tissues were dissected and immediately frozen on dry ice.

Sodium dodecyl sulfate–polyacrylamide gel electrophoresis (SDS-PAGE) was performed according to the method of Laemmli (1970) using gels 8 cm in length with acrylamide gradients of 4–20%. Proteins were transferred to nitrocellulose membranes as described by Towbin et al. (1979). Membranes were treated overnight with 3% nonfat dry milk in TBS-Tween (50 mM Tris, 150 mM NaCl, pH 7.4, with 0.05% Tween 20). Anti-NR1 antibodies were used at 0.2 μg/ml, and detection of bound antibody was done using the ECL chemiluminescence detection system (Amersham, Arlington Heights, IL). For controls, antibodies were preincubated overnight with the peptide at 0.2 mg/ml. Prestained standards from GIBCO–Bethesda Research Labs were myosin, phosphorylase B, BSA, ovalbumin, and α-chymotrypsinogen, migrating at M_r = 210 K, 103 K, 71 K, 46 K, and 25 K, respectively. Molecular weights were estimated using unstained standards, myosin (200 kDa), β-galactosidase (116 kDa), phosphorylase B (97 kDa), BSA (66 kDa), and ovalbumin (45 kDa), obtained from Bio-Rad (Richmond, CA).

Tissue preparation. Young male Sprague–Dawley rats (120–250 gm) were anesthetized with 20% urethane and perfused transcardially, as described previously (Petralia and Wenthold, 1992), with 0.12 M phosphate buffer (pH 7.2) followed by 4% paraformaldehyde in the same buffer, with or without 0.1% glutaraldehyde for light/electron or light microscopy, respectively. In most cases, about 0.5 ml of 1% sodium nitrite in 0.012 M phosphate buffer was injected into the left ventricle just prior to perfusion. Brains and other organs were removed and postfixed in the same fixative for 1 hr at 4°C, washed three times in cold phosphate-buffered saline (PBS; 0.9% NaCl in 7 mM phosphate buffer, pH 7.4) over 1 hr, and then either sectioned immediately or placed overnight at 4°C in PBS. Tissues were sectioned in cold PBS with a microslicer (Pelco DTK-3000W) at 50 μm. Organs other than the brain were embedded in 1 % agarose in PBS as a supportive material for sectioning.

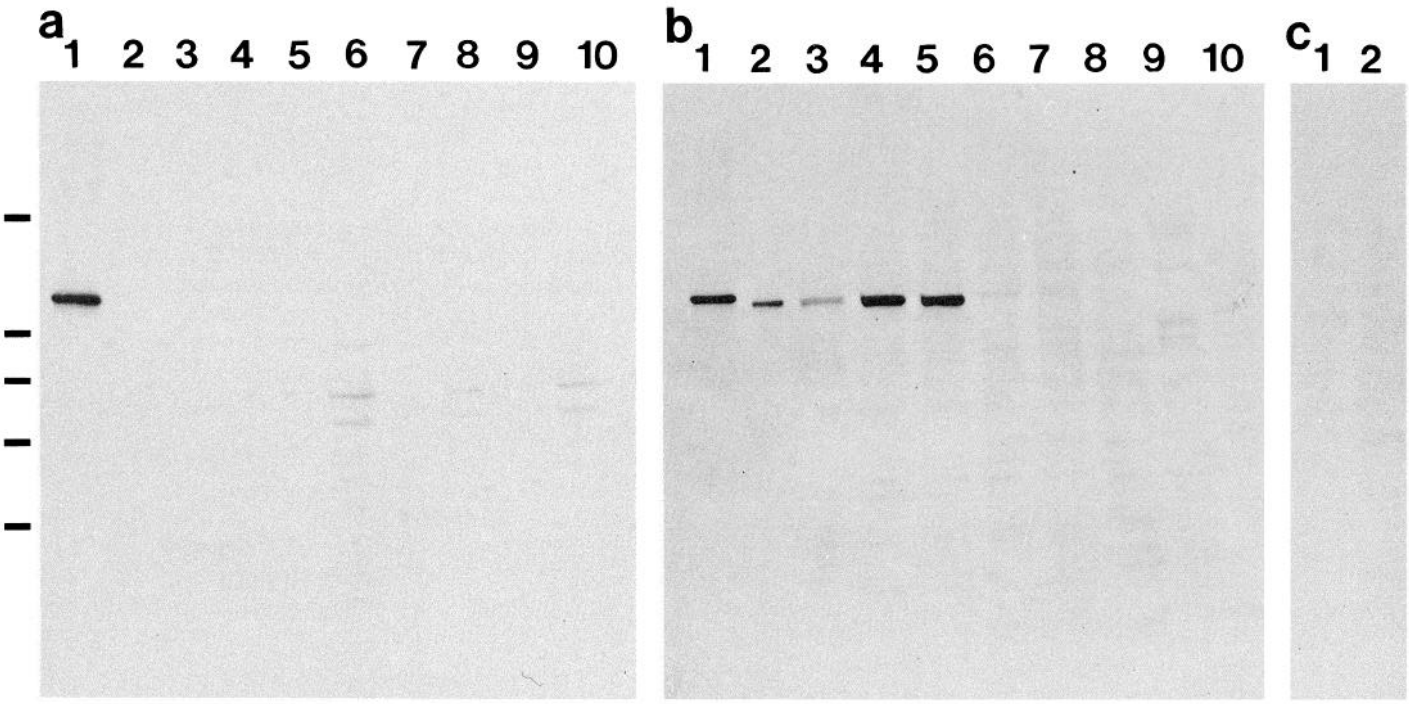

Figure 1. Immunoblot analysis of SDS-PAGE gels of transfected cell membranes and rat tissues. *a,* HEK-293 cell membranes transfected with NMDAR1 (*1*), GluR1 (*2*), R2 (*3*), R3 (*4*), R4 (*5*), R5 (*6*), R6 (*7*), R7 (*8*), KA1 (*9*), and KA2 (*10*). *b,* HEK-293 cell membranes transfected with NMDAR1 (*1*), postsynaptic densities (*2*), olfactory bulb (*3*), cerebral cortex (*4*), hippocampus (*5*), superior colliculus (*6*), cerebellum (*7*), liver (*8*), skeletal muscle (*9*), and kidney (*10*). *c,* Antibody pretreated with peptide. HEK-293 cell membranes transfected with NMDAR1 (*1*) and cerebral cortex (*2*). For analysis of rat tissues, 30 μg of protein was applied to each well; 2 μg was applied for the postsynaptic density sample. *Bars* show the positions of prestained standards: myosin (*top*), phosphorylase B, BSA, ovalbumin, and α-chymotrypsinogen (*bottom*).

Immunocytochemistry. The most useful antibody concentrations were between 2 and 4 mg/ml. The preembedding immunocytochemical procedure has been described in detail in Petralia and Wenthold (1992). Briefly, sections were incubated in 10% normal goat serum in PBS for 1 hr and then kept overnight in the primary antibody (AbT3) in PBS. The next morning, after washing in PBS, sections were incubated in biotinylated secondary antibody for 1 hr, washed, incubated in avidin–biotin–peroxidase (Vectastain kit, Vector Laboratories, Burlingame, CA), washed, treated with 3′,3-diaminobenzidine tetrahydrochloride (10 mg/20 ml PBS + 5 ml of 30% hydrogen peroxide), and washed. Sections for light microscopy were mounted on slides and coverslips were attached with Permount. Sections for electron microscopy were fixed in 1% osmium tetroxide in PBS for 1 hr, washed, dehydrated, and embedded in Poly/BED 812 resin (Polysciences, Inc., Warrington, PA). Yellow to light gold sections (average 75 nm) were taken from the edge (i.e., perpendicular to the plane of the section) of the 50 μm sections on an LKB Ultratome IV ultramicrotome, and examined unstained in a JEOL JEM-100CX II transmission electron microscope.

Controls. Sections in which PBS was substituted for the primary antibody (PBS controls) were run in every experiment for both light and electron microscopy. In addition, preadsorption controls were run at the highest antibody concentration used (4 μg/ml). Three tubes [(1) primary antibody; (2) primary antibody plus 50 μg/ml (final concentration) of glutaraldehyde-treated BSA; (3) primary antibody plus 50 μg/ml of the specific peptide, conjugated to BSA with glutaraldehyde] were set at 4°C for 24 hr, centrifuged, and incubated with sections, which were processed as described above. A preadsorption control using 2.5 μg antibody/ml PBS with specific peptide alone or conjugated to BSA with glutaraldehyde was also tested, using sections from another rat.

Anatomical survey. Sagittal sections from 14 sides of eight rats and coronal sections from four rats were examined. Sagittal sections were taken from up to six levels (PW79–PW85, i.e., corresponding to Figs. 79–85 in Paxinos and Watson, 1986). Coronal sections were taken from up to 13 different levels, corresponding to figures of Paxinos and Watson. Typically, the angle of our coronal sections was oblique to those of PW such that the dorsal portion of a section corresponded to a PW figure number 3 or 4 higher than the ventral portion. Transverse sections were examined from the cervical spinal cords of seven rats. In addition, sections were taken at arbitrary angles of pineal glands and cervical dorsal root ganglia (several per animal) from three and six rats, respectively, and from a plane parallel to the dorsal surface of pituitary glands of five rats. Thin sections for electron microscopy of cerebral cortex, hippocampus, and cerebellum were taken from sagittal vibratome sections corresponding to PW82–PW85 from two rats. Thin sections of the cerebral cortex were taken perpendicular to the long axis of the cortex so that usually all layers were represented in the thin sections. Thin sections of the hippocampus were taken from the rostral end. Thin sections of the cerebellum were taken perpendicular to the long axis of a lobule.

Choice of antibody concentrations was based on the lowest antibody concentration where dense staining was present in some structures as compared to PBS control sections. Level of staining was based on an arbitrary relative scale where the densest stained structures were assigned a value of 4, and structures in which staining was not higher than the PBS control sections were assigned a value of 0 (see Appendix). Unless otherwise stated, these values reflect the overall staining pattern including neuronal and neuropilar staining as defined in the results. Descriptions of neuron structural types are based on the staining pattern of those neurons, and it is understood that some descriptions could be misleading if major portions of the cell were not evident due to lack of staining or were obscured by denser staining in the surrounding neuropil. Described neuron types include round, ovoid, multipolar (where the shape of the cell is not distinctly oriented in a particular direction), elongate ovoid or multipolar (where the shape of the cell is mainly ovoid or multipolar but is distinctly oriented in one direction), fusiform (i.e., very elongate and spindle-shaped), and elongate (an elongate cell that is not distinctly fusiform). Of course, usually cell shape was not absolute and the shape term used to describe neurons in each brain structure reflects the best choice for the majority of cells.

Sections stained with antibody to NMDAR1 were compared to sections stained with antibodies to AMPA receptors, that is, GluR1, -2/3, and -4. These included sections (mainly of GluR1) prepared with many

of the experiments described above, as well as sections prepared for the previous study (Petralia and Wenthold, 1992). Only findings that have not been described in the latter article are mentioned in the results.

Results

Specificity of anti-NMDAR1 antibody

Immunoblot analysis of membranes from HEK-293 cells transfected with NMDAR1 showed a single band that migrates at M_r estimated to be 120,000 (Fig. 1*a*). This size is consistent with the calculated molecular weight of 105,500 (Moriyoshi et al., 1991); the difference in sizes is most likely due to glycosylation of the mature protein since multiple potential glycosylation sites are present on the molecule. Deglycosylation has been shown to reduce the size of the major NMDAR1 immunoreactive band in transfected cells (Chazot et al., 1992). The antibody did not cross-react with several glutamate receptors of the AMPA and kainate subtypes. Analysis of brain tissues showed a major immunoreactive band migrating slightly ahead of the immunoreactive band from transfected cells. This dissimilarity in apparent molecular weight could arise from a slight difference in glycosylation. Antibodies also were made to the NMDAR1 N-terminus and to an internal site (not described here), and these antibodies also showed the immunoreactive band from the brain migrating slightly ahead of that from transfected cells. In some cases, for example the olfactory bulb (Fig. 1*b*, lane 3), the immunoreactive band may be made up of at least two slightly separated bands that may reflect different degrees of glycosylation or splice variants of the NMDAR1 subunit (Durand et al., 1992; N. Nakanishi et al., 1992; Sugihara et al., 1992). Dense staining was seen in bands from cerebral cortex and hippocampus, while staining in the olfactory bulb was moderate and that in the cerebellum and superior colliculus was light. Labeling was not seen in non-neuronal tissues, including liver, skeletal muscle, and kidney.

Light microscopy—controls

Sections in which PBS was substituted for the primary antibody (AbT3) were usually very light and never showed evidence of specific staining. Similarly, no specific staining was seen in sections exposed to antibody that was preadsorbed to BSA-conjugated peptide, except for a light staining in the dorsal root ganglion cells and pineal gland. However, compared to PBS control sections, background staining was a little higher in some structures, including the motoneurons of laminae IX and neuropil of laminae I and II of the spinal cord, granular layer of the cerebellum, and supraoptic, pontine, motor V, facial, lateral reticular, spinal trigeminal, and superficial dorsal cochlear nuclei. Background staining was slightly darker in preadsorption controls with peptide alone as compared to controls with BSA-conjugated peptide. In contrast, BSA controls and experimental sections run at the same time and under similar conditions stained normally, that is, the same as with other experimental sections.

Light microscopy—general

At low magnifications (Figs. 2, 3), staining with antibody AbT3 appeared to be highest in the hippocampus, but was high also in the deep cortex, olfactory structures, caudate-putamen, thalamus, cerebellum, and parts of the caudal brainstem (see Appendix). At higher magnifications, it was evident that the staining patterns in different structures varied. Staining will be described as "neuropilar" and "neuronal," as defined in Petralia and Wenthold (1992); that is, neuronal staining refers to staining of the cell body, excluding nucleus, and the major dendrites, which could be traced from the cell body, while neuropilar staining includes processes not traced to specific cell bodies and the unresolvable matrix between cells. Puncta were seen on stained neurons and neuropil and were more prominent and numerous in the denser-stained structures. Their presence is noted only in structures where they are particularly prominent. The pattern of neuronal staining was variable, even within the same neuronal cell group; some neurons showed a diffuse stain throughout the cytoplasm, and others showed a coarse, granular staining in the cell body and/or a concentration of stain in one pole of the cell body. Dendrites of some neurons stained as dense as the cell body, while in other neurons the cell body stained denser than the dendrites. Examples are noted in the text where a particular neuronal staining pattern is most evident. Sometimes considerable variation was seen in staining density in groups of neurons. A few lightly stained cells in a group of similar, densely stained cells can be attributed to reduced staining in the deep portions of the 50 μm sections. However, substantial numbers and/or aggregations of lighter-stained cells may be significant, and the most definitive examples are mentioned in the text.

Cortex

In general, overall staining in the isocortex and allocortex was moderate (Figs. 2, 3, 4*a,b*; Appendix). Immunostaining of the cerebral cortex varied slightly with the region (Appendix). In sagittal sections (PW82) proceeding from rostral to caudal, neuropilar staining was moderate in the claustrum, light to moderate in the lateral orbital cortex, and light to moderate in frontal cortex, area 2, with moderately dense staining in layer 2. Staining of neurons in layer 2 of the frontal cortex, area 2, was similar to that of neurons of layer 5, ranging from moderate to dense. In contrast, neuronal staining of layer 5 was noticeably denser than that of the outer layers in most other areas of the cortex as seen in sagittal sections. Examination of the forelimb/hindlimb area (Figs. 2, 4*b*) in more detail revealed little or no staining in cells of layer 1, moderate neuropilar stain and little or no neuronal staining in layer 4, and moderately dense neuronal staining in layers 2, 3, and 6. Densest stain was found in many of the pyramidal neurons of layer 5 (Fig. 4*b*) and horizontal neurons of the ventral portion of layer 6. Staining in nonpyramidal cells of layer 5 was comparatively light. In coronal sections (PW27–PW29) containing, from the midline, the retrosplenial granular and agranular areas, areas 1 and 2 of the frontal cortex, hindlimb area, areas 1 and 2 of the parietal, and the perirhinal cortex, overall staining was similar to that in sagittal sections. Densest staining was seen in many of the pyramidal neurons of layer 5, with more in parietal area 1 than in 2, and with the densest stained pyramidal cells in the retrosplenial agranular cortex. The largest and densest puncta were seen in layer 6 of the frontal cortex (areas 1 and 2). In all areas of isocortex, little or no staining was seen in neurons of layer 1 and moderately dense staining was seen in many neurons of layers 2 and 3, as seen in sagittal sections. In both sagittal and coronal sections, neurons of layer 4 usually had little or no staining. However, in rostral parietal sections, layer 4 contained large, ovoid patches of moderately stained neuropil (Fig. 4*a*), which may correspond to rat barrel fields (e.g., Welker and Woolsey, 1974; Jaarsma et al., 1991). Also, overall staining in adjacent layers 2 and 3 was denser in this area than that of layers 5 and 6. In comparison, no particular staining pattern was ev-

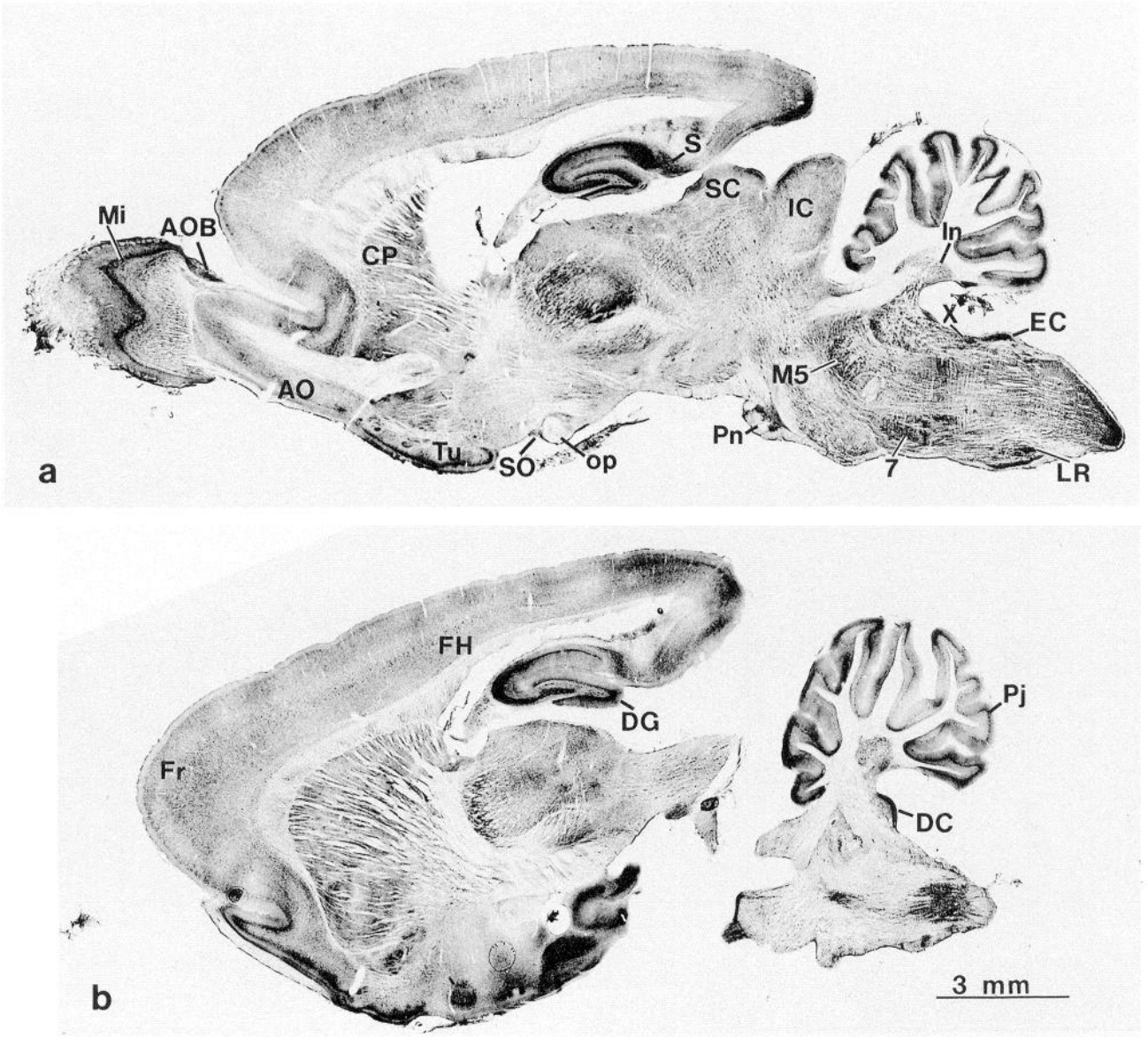

Figure 2. Low magnifications of sagittal sections immunolabeled with antibody to NMDAR1. *a,* Corresponds most closely to Figure 81 of Paxinos and Watson (1986, PW81). *b,* More lateral than *a,* corresponding most closely to PW83–PW84. Magnification, 6.6×. Abbreviations used in Figures 2 and 3: *AO,* anterior olfactory n.; *AOB,* accessory olfactory bulb; *Ar,* arcuate hypothalamic n.; *Bl,* basolateral amygdaloid n.; *C,* cuneate n.; *cc,* corpus callosum; *CP,* caudate-putamen; *DC,* dorsal cochlear n.; *DG,* dentate gyrus; *DH,* outer dorsal horn; *DL,* lateral geniculate n., dorsal part; *EC,* external cuneate n.; *FH,* forelimb/hindlimb area of cortex; *Fr,* frontal cortex; *G,* gracilis n.; *H,* habenula; *IC,* inferior colliculus; *IO,* inferior olive; *Ip,* interpeduncular n.; *In,* interposed cerebellar n.; *LA,* lateral amygdaloid n.; *LD,* lateral septal n., dorsal part; *LR,* lateral reticular n.; *LV,* lateral vestibular n.; *Mi,* mitral cell layer of olfactory bulb; *MG,* medial geniculate n.; *Mn* motoneurons of ventral horn; *M5,* motor trigeminal n.; *op,* optic tract; *Pi,* piriform cortex; *Pj,* Purkinje cell layer of cerebellum; *Pn,* pontine n.; *P1,* parietal cortex, area 1; *R,* red n.; Rt, reticulothalamic n.; *S,* subiculum; *SC,* superior colliculus; *SN,* substantia nigra; *SO,* supraoptic n.; *S5,* spinal trigeminal n.; *S5C,* spinal trigeminal n., caudal part; *Tu,* olfactory tubercle; *VC,* ventral cochlear n.; *VL,* lateral geniculate n., ventral part; *X,* nucleus X; *3,* oculomotor n.; *7,* facial n.; *8,* auditory nerve; *12,* hypoglossal n.; *III,* third ventricle; *IV,* fourth ventricle. In all light microscope figures (2–10), dorsal is to the top and rostral is to the left (sagittal sections) unless otherwise stated. The uneven staining seen in some parts of the cerebral cortex (and probably cerebellar cortex, as well) of Figures 2 and 3 is an artifact of the immunostaining procedure.

ident in layer 4 of this area in adjacent sections stained with antibody to GluR1.

Olfactory regions

Immunostaining of neuropil in the main olfactory bulb was light in the glomerular layer, moderate in the external plexiform layer, light to moderate in the internal plexiform layer, and moderate in the granule cell layer (Figs. 2*a*, 4*c,d*). Moderately dense staining was seen in mitral cells (Fig. 4*c,d*). In contrast, only moderate staining was evident in most other neurons, including short axon cells of the upper granule cell layer; small to large, round to elongate cells of the external plexiform layer; and periglomerular neurons (Fig. 4*c,d*). However, a few neurons in each of these layers were stained moderately densely. Compared to the main olfactory bulb, the accessory olfactory bulb (Fig. 2*a*, Appendix) had lighter staining in the glomerular layer and slightly denser

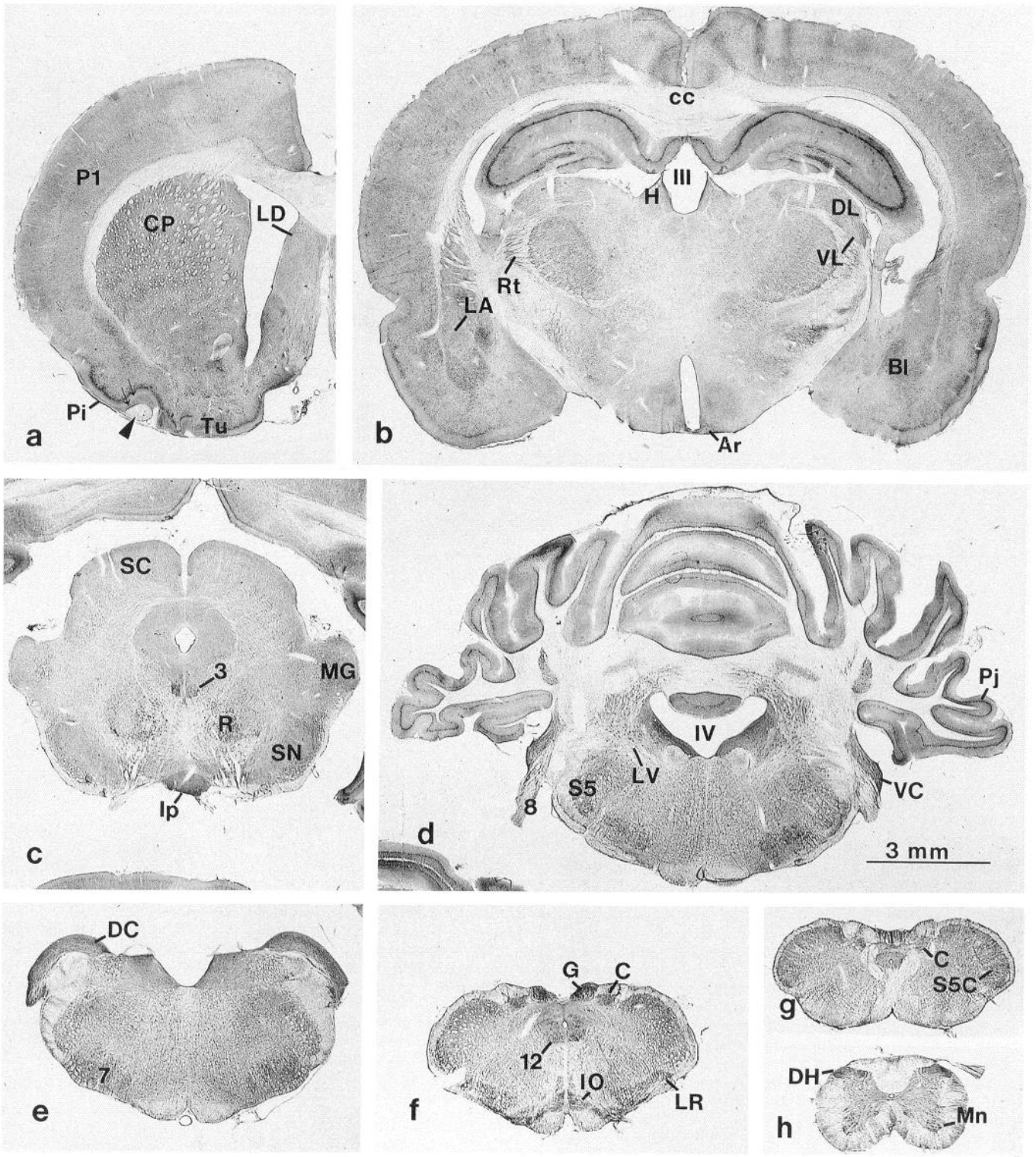

Figure 3. Low magnifications of coronal sections immunolabeled with antibody to NMDAR1, arranged from rostral forebrain (*a*) to cervical spinal cord (*h*). *Arrowhead* in *a* indicates lateral olfactory tract; *small arrows* indicate layers Ia (outer) and Ib (inner) of the piriform cortex. Abbreviations are as in Figure 2. Magnification, 7.1×.

staining in the granule cell layer. Staining of neurons of the external plexiform layer of the accessory olfactory bulb was similar to that of the mitral cells of the main olfactory bulb. Most neurons of the anterior olfactory nucleus (Fig. 2*a*) were stained moderately densely. A few of the elongate, multipolar neurons of the dorsocaudal portion were stained very densely. Neurons of the olfactory tubercle were stained lightly to moderately, and neuropilar staining ranged from light to moderately dense, depending on the layer. Layer Ia of the piriform cortex (Fig. 3*a*) stained moderately in contrast to layer Ib, which con-

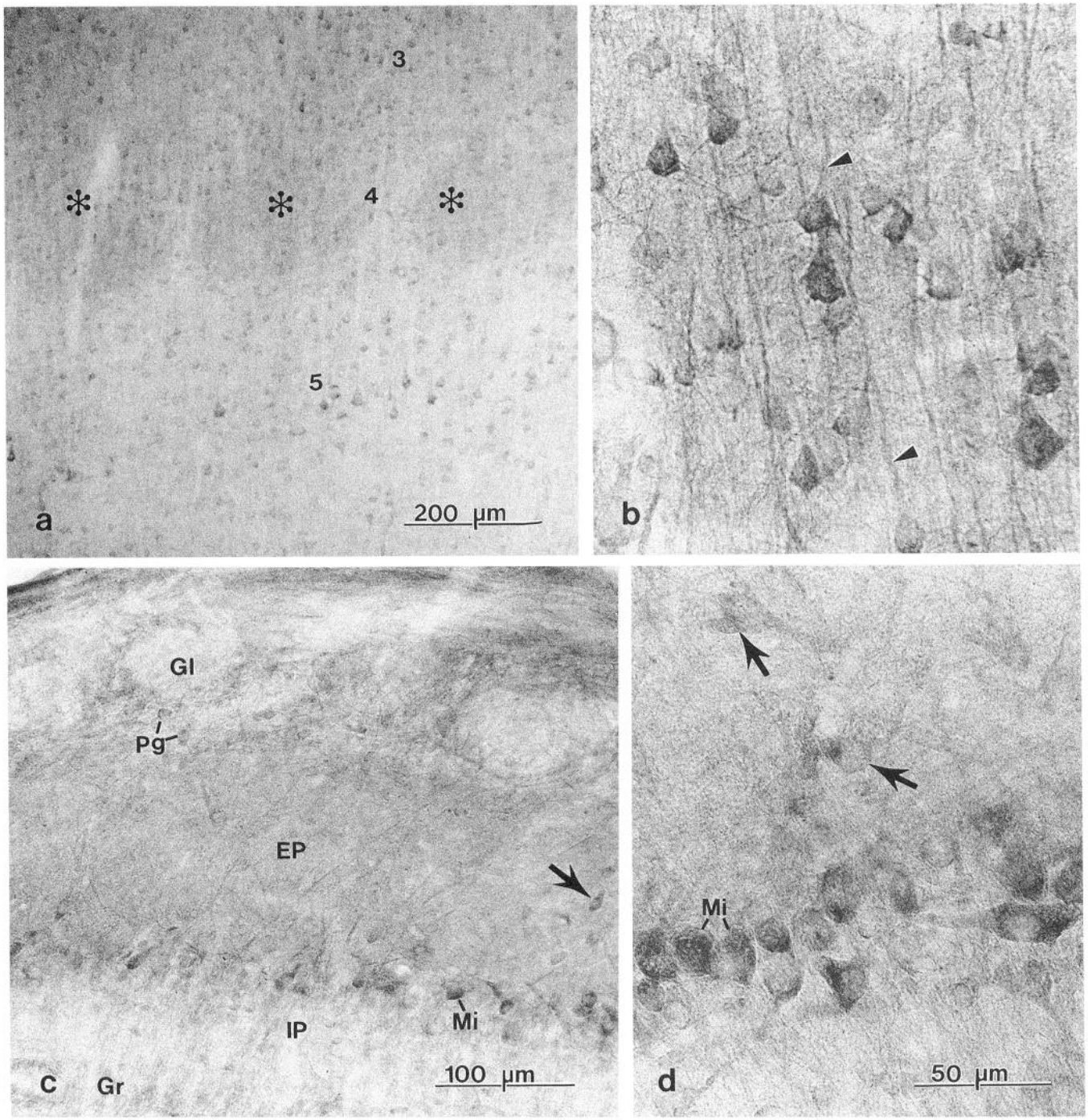

Figure 4. Cerebral cortex and olfactory bulb. *a,* Coronal section of rostral parietal cortex, area 1 (corresponds to the level of Fig. 3*a*). Note barrel fields (*asterisks*) in layer 4. *3–5*, layers 3–5. *b,* Sagittal section of layer 5 of forelimb/hindlimb cortex. *Arrowheads*, apical dendrites of pyramidal cells. *c* and *d*, High and low magnifications of sagittal sections of olfactory bulb. *c* was taken from the ventral part of the olfactory bulb and has been oriented with dorsal to the bottom for ease of comparison. *Gl*, glomerular layer; *Gr*, granule cell layer; *IP* and *EP*, internal and external plexiform layers; *Mi*, mitral cell; *Pg*, periglomerular cell. *Arrows*, cells of external plexiform layer. Magnification: *a,* 112×; *b* and *d,* 447×; *c,* 226×.

tained little or no staining. A similar staining pattern was seen with antibodies to GluR1–GluR4, with layer Ia much denser than layer Ib.

Hippocampus

Very dense staining was seen in the pyramidal neurons of CA1–CA3, and in neurons of the hilus. Staining varied from moderate to very dense in various neurons of the stratum oriens (i.e., outer layer of CA1–CA3; Figs. 2, 3, 5). The latter neurons were most common in the most peripheral portion of the stratum oriens of CA1 (Fig. 5*d*). In addition, lightly or moderately stained neurons were seen occasionally in the molecular layers of the hippocampus proper (Fig. 5*d*) and dentate gyrus. In lateral sagittal sections, staining was noticeably denser in the neuropil of the stratum lucidum, that is, the region of the proximal portions of the apical dendrites of the CA3 pyramidal cells, as compared

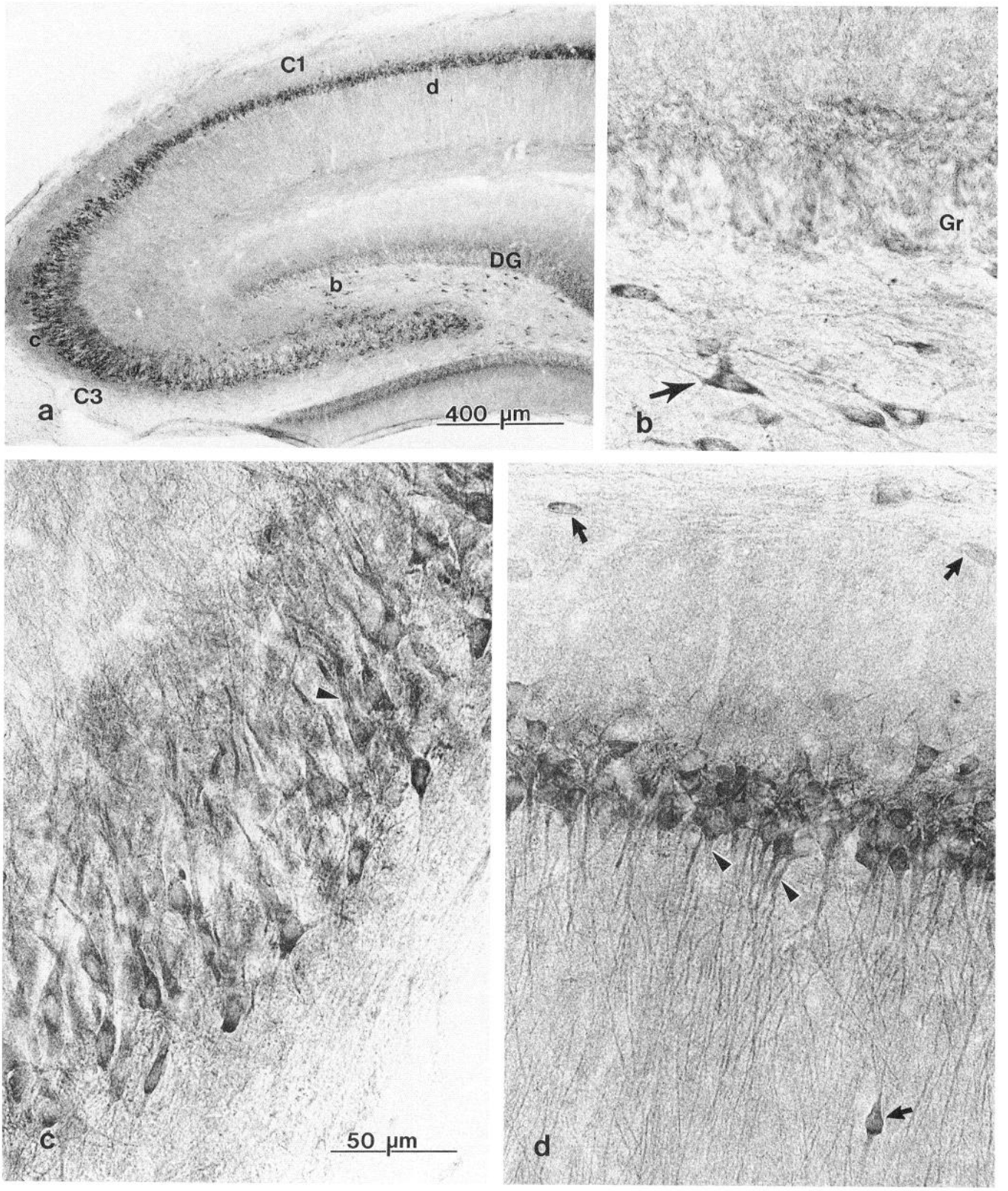

Figure 5. Sagittal section of hippocampus. *a,* Low magnification of rostral two-thirds of hippocampus. *Areas labeled b–d* are shown at higher magnifications in *b–d. b,* Dentate gyrus. *c,* CA3 region. *d,* CA1 region. *C1* and *C3*, CA1 and CA3 regions; *DG*, dentate gyrus; *Gr*, granule cells of dentate gyrus. *Large arrow*, hilar cell; *small arrows*, nonpyramidal cells; *arrowheads*, apical dendrite of pyramidal cells. Magnification: *a,* 56×; *b–d,* 447×.

to the distal portions (Fig. 5*a*). In contrast, in the most medial sagittal sections, this denser band of stain was limited more to the CA2 region. In rostral coronal sections, an equivalent band of neuropilar staining was seen in the medial CA3 region (i.e., portion closest to hilus; also called CA3c, CA4, or proximal CA3; reviewed by Bayer, 1985; Brown and Zador, 1990; Ishizuka et al., 1990), while the neuropil surrounding the moderately stained, proximal portions of apical dendrites of pyramidal cells of the lateral CA3 region usually was unstained. The former stained neuropil of the medial CA3 appeared to be formed into horizontal bands of staining. In very caudal sections, these bands of staining extended into the lateral CA3. A similar pattern of staining in the CA2–CA3 region could be seen with antibody to GluR2/3 and a similar but lighter staining pattern with antibody to GluR4. In contrast, this staining pattern was never seen with antibody to GluR1. Staining in the granular layer of the dentate gyrus was light to moderate (Fig. 5*b*). Densest staining of the dentate gyrus was found at the boundary of the granular and molecular layers, and in the proximal third of the molecular layer (Fig. 5*a,b*). This is the location of terminals derived from axons of hilar neurons of both ipsilateral and contralateral dentate gyri (Amaral, 1987; Brown and Zador, 1990). A similar but less distinctive difference between proximal and distal parts of the molecular layer could be seen with antibody to GluR2/3, but the difference was not readily discernible with antibodies to GluR1 or -4.

Both neuropil and the medium, round to ovoid neurons of the induseum griseum stained moderately to moderately densely. Staining of the tenia tecta was similar to that of the induseum griseum but neuronal staining was denser on average.

Amygdala and septum

Neuropilar staining in most areas of the amygdaloid complex (Fig. 3*b*, Appendix) was light. Most neurons, which were mostly ovoid but also included some round and some elongate neurons, stained moderately. The lateral septal nucleus (Fig. 3*a*) contained light to moderate, multipolar and dorsoventrally elongate neurons in a lightly stained neuropil. Neuropilar staining in the septohippocampal nucleus was moderate, and the dorsoventrally elongate, medium neurons stained lightly to moderately.

Basal ganglia

Staining in the compact portion of the substantia nigra (Fig. 3*c*, Appendix) was moderate in the neuropil and moderate to dense in many neurons, which were mostly multipolar in shape. Staining was light in the neuropil of both the lateral portion and much of the reticular portion of the substantia nigra, and was dense in many neurons, which were mostly elongate–multipolar. Neuropilar staining of the ventralmost part of the reticular portion was denser than other parts. In all portions of the substantia nigra, neurons tended to be stained more densely on one pole of the cell. Neuron staining in the caudate-putamen (Figs. 2, 3*a*, 6*a*) ranged from light to moderately dense in a moderately stained neuropil. Moderately densely stained cells included mainly medium-sized, round to multipolar neurons, and occasional large, elongate neurons. Neuronal staining was variable with substantial cytoplasmic staining often confined to the cell body, and staining of most dendrites confined to puncta. Staining of the nucleus accumbens was similar to that of the caudate-putamen, although stained neurons were generally smaller on average in the former. Neuropil and most neurons of the globus pallidus stained lightly. However, some groups of the medium to large, multipolar neurons stained moderately to moderately densely. Staining in the small to medium-sized neurons of the ventral pallidum varied from light to moderate, although a few were moderately dense, and the neuropil was light. Small stained neurons were ovoid to fusiform while medium-sized cells were mostly multipolar. The ovoid, small cells of the substantia innominata had little or no staining, although a few were stained moderately. Neuropil was light in the latter and light to moderate in the adjacent nucleus of the horizontal limb of the diagonal band, which in sagittal sections contained mostly multipolar medium-sized cells and ovoid to rostrocaudally fusiform smaller cells, with staining varying from moderate to moderately dense. In coronal sections, stained neurons were mainly multipolar although some were mediolaterally elongated. The moderately stained neuropil of the vertical limb of the diagonal band was restricted to narrow vertical strips. Staining of the small to medium, round, polygonal, or occasionally dorsoventrally elongate cells varied from light to moderately dense. The neuropil of the subthalamic nucleus was fairly uniform and moderately stained. Small- to medium-sized neurons were stained moderately, but showed dense punctate staining on the peripheries of the cell bodies.

Epithalamus and thalamus

In the epithalamus, staining of neuropil was moderate in the lateral and moderately dense in the medial habenula (Fig. 3*b*). Most of the small and large neurons of the lateral habenula contained little or no staining, while neurons of the medial habenula were not evident. Overall staining of the pineal gland was moderate to moderately dense (Appendix), although individual cell staining was obscure. In addition, there were a few scattered cell processes and occasional cell bodies stained densely in some sections.

The densest-staining neurons in the thalamus were found in the ventral nuclear group, including the ventrolateral, ventromedial, and ventroposterolateral nuclei (Appendix). Neurons of the ventrolateral nucleus were mostly medium sized and multipolar, and most were moderately densely to densely labeled, while the surrounding neuropil stained moderately. The overall staining pattern was similar in the ventral posteromedial and posterolateral (Fig. 6*b*) nuclei, although neurons in the former stained somewhat less densely than in the ventrolateral nucleus. The ventromedial nucleus contained moderately to densely stained, small to medium multipolar neurons; lightly to moderately stained, large multipolar neurons; and a lightly stained neuropil. Neuropilar staining in the lateral nuclear group, including the lateral dorsal and lateral posterior nuclei, was light. These two nuclei differed in the staining of their neurons, which included small to medium multipolar types. Those of the lateral posterior nucleus were moderately to moderately densely stained, while most of those of the lateral dorsal nucleus were lightly stained. Dorsomedial and ventrolateral portions of the anteroventral nucleus stained similarly, with light to moderate staining of the neuropil and mostly moderate staining in the very small to small ovoid cells, which were elongated along dorsoventral fiber tracts. In the reticulothalamic nucleus (Figs. 3*b*, 6*b*), the moderately stained, multipolar to fusiform neurons, which occasionally bore distinct puncta, were arranged in groups of four or five cells surrounded by moderately stained neuropil, with lighter-stained neuropil between the patches. Staining of neuropil of the zona incerta was light to moderate. The moderately

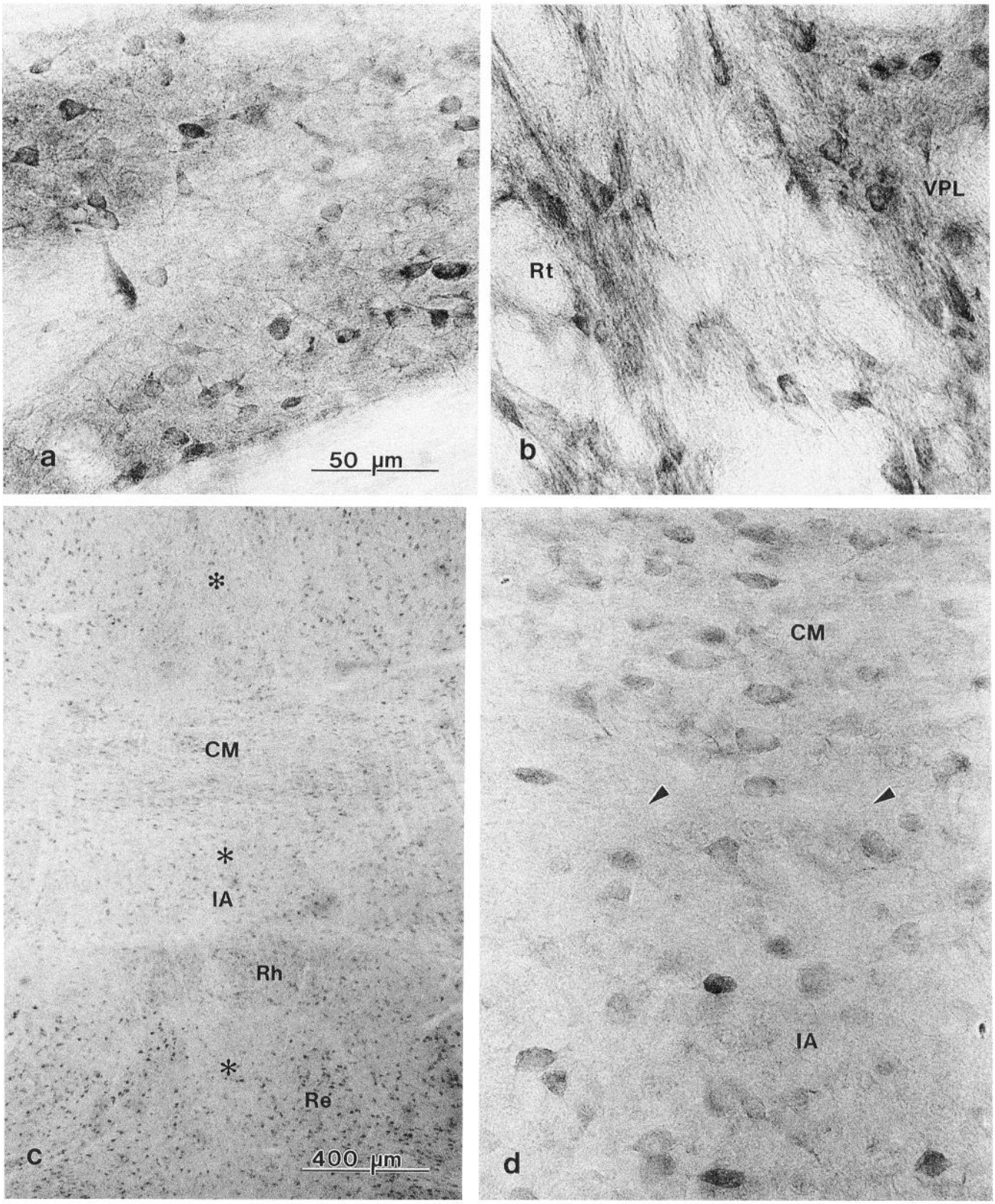

Figure 6. Striatum and thalamus. *a,* Sagittal section of caudate-putamen. *b–d,* Coronal sections of thalamus. *b,* Border between reticulothalamic (*Rt*) and ventral posterolateral nuclei (*VPL*). *c,* Midline thalamic nuclei. *CM*, central medial thalamic n.; *IA*, interanteromedial thalamic n.; *Rh*, rhomboid n.; *Re*, reuniens n. *Asterisks*, midline. *d,* High magnification of the border (*arrowheads*) between the central medial and interanteromedial thalamic n. Magnification: *a, b,* and *d,* 447×; *c,* 56×.

to densely stained, small to medium neurons included multipolar, rostrocaudally elongated, and fusiform types.

In the nuclei of the midline region (PW26), neuropilar staining was light in the central medial, anteromedial, interanteromedial, and reuniens nuclei, while it was moderate in the anterior paraventricular and rhomboidal nuclei (Fig. 6*c,d*). Most of the small to medium neurons in these areas were lightly stained or unstained. In contrast, moderately to moderately densely stained medium multipolar neurons were common in the lateral parts of the reuniens nucleus.

Immunostaining was similar in dorsolateral and ventrolateral geniculate nuclei (Fig. 3*b*) with neuropil varying from light in more medial portions and moderate in more lateral portions. The small to medium, ovoid to multipolar cells contained little or no stain, except for a moderate staining in some of the more lateral cells. Neuropil of the medial geniculate nucleus (Fig. 3*c*) stained lightly to moderately. Staining was light in the mostly small cells of the dorsal and ventral parts, with the dorsal part containing the most stained cells. The suprageniculate and medial parts contained small to large, lightly to moderately stained, ovoid to bipolar cells (neurons of the medial part surrounded bundles of axons).

Hypothalamus and pituitary gland

In sagittal sections (PW81), neuropil was light in the presumptive lateral preoptic area and most neurons showed little or no staining, although a few round to multipolar, medium-sized neurons stained moderately. In contrast, neurons of the adjacent lateral hypothalamic area stained moderately densely to densely in a lightly to moderately stained neuropil. Stained neurons were mostly small to medium and ovoid to rostrocaudally elongate. In the presumptive medial tuberal nucleus, neuropil was light and most neurons contained little or no staining. However, a few large, multipolar neurons were moderately to densely stained. In coronal sections (Fig. 3*b*), staining of neuropil of the arcuate nucleus was moderately dense but neurons were not evident.

The most notable staining in the hypothalamus was found in groups of neurons that belong to the hypothalamo-neurohypophysial system (reviewed by Armstrong, 1985), including mainly neurons in the supraoptic and paraventricular nuclei (Fig. 7*a–c*). Staining in the medium to large ovoid neurons of the supraoptic nucleus was among the densest in the brain (Fig. 7*b*). Most neurons were stained densely to very densely, although some were stained moderately as was the neuropil. Similar staining was seen in the ovoid to elongate neurons of the retrochiasmatic portion of the supraoptic nucleus (Fig. 7*c*). Neuropilar staining varied from moderate along the pial surface to light in deeper portions of the nucleus. In addition, similar densely stained neurons were found scattered in the dorsocaudal regions of the hypothalamus extending rostral to the level of the optic chiasm, as seen in sagittal sections (PW80–PW81). Some of these appeared to be located in the nucleus of the stria medularis, and a few of them were found as single neurons in the more dorsal portion of the stria medularis. One group seen in coronal section consisted of a small cluster of neurons surrounding a blood vessel. Also, a few appeared to be scattered singly in the zona incerta and in the lateral hypothalamic area, along the dorsal border of the supraoptic decussation. The lateral magnocellular division of the paraventricular nucleus (Fig. 7*a*) contained neurons stained similarly to those of the supraoptic nucleus. These neurons were similar in shape but appeared to be slightly smaller on average than those of the supraoptic nucleus. In contrast, other adjacent parts of the paraventricular hypothalamic nucleus contained a few small to medium cells that stained lightly to moderately. Some parts including the medial magnocellular portion were not examined.

In general, the median eminence stained moderately densely, although cells were obscure. The ependymal lining of the median eminence stained densely. In contrast, the adjacent ependymal lining of the ventricular surface of the hypothalamus contained little immunolabeling.

Overall moderate staining was seen in anterior and posterior lobes of the pituitary gland, while the intermediate lobe stained moderately densely. In addition, the anterior lobe typically contained scattered moderately densely stained coarse-grained cells (Fig. 7*d*).

Brainstem—sensory

Visual system. In the superior colliculus (Figs. 2*a*, 3*c*), neuropilar staining was moderate in the zonula and superficial gray, and the former contained a few moderately stained small, ovoid cells as seen in both coronal and sagittal sections. The optic nerve layer contained moderately stained bands between the unstained fiber bands. The stained bands contained a few scattered, medium multipolar neurons that were stained lightly to moderately, typically in only one portion of the cell body. Most of the small, ovoid neurons of the intermediate gray were stained lightly or were unstained, although an occasional larger cell was stained moderately densely. Bands of neuropil in the intermediate white layer were stained lightly to moderately and contained many stained small to large cells, of which the most prominent were the large, moderately to densely stained multipolar neurons (Fig. 8*a*). Presumably, the latter belong to the group of large, multipolar neurons associated with the adjacent lateral deep gray described by Tokunaga and Otani (1976). Staining in the neuropil of the deeper portions of the superior colliculus was moderate and contained lightly and occasionally moderately stained small, dorsoventrally elongate cells.

Most of the cells of the parabigeminal nucleus contained little or no staining, although some stained moderately. Stained cells varied from small ovoid to medium, dorsoventrally elongate ovoid.

Vth cranial nerve. Both neuropil and the mostly small- to medium-sized cells of the principle sensory nucleus of the trigeminal nerve were stained lightly to moderately. However, patches of medium-sized, moderately dense, multipolar neurons, some of them rostrocaudally elongate, were found, especially in the most dorsal and ventral regions. Larger stained neurons were seen occasionally in the dorsomedial portion of the nucleus. In both sagittal and coronal sections, the most rostral portion (i.e., oral portion) of the spinal trigeminal nucleus (Fig. 3*d*) contained mostly small to medium, lightly to moderately stained multipolar neurons in a moderately stained, punctate neuropil. In addition, there were a few large, moderately densely to densely stained, multipolar neurons. Just caudal to this portion was an extensive region, presumably corresponding to the interpolar portion (Tracey, 1985), containing many densely stained, large multipolar neurons, which included some of the densest stained neurons of the lower brainstem. In sagittal sections, the major dendrites of many of these neurons were oriented dorsoventrally along fibers running perpendicular to the horizontal bands of moderately stained neuropil that contained many puncta. In addition, this portion contained small- to medium-sized cells stained lightly to moderately. The caudal

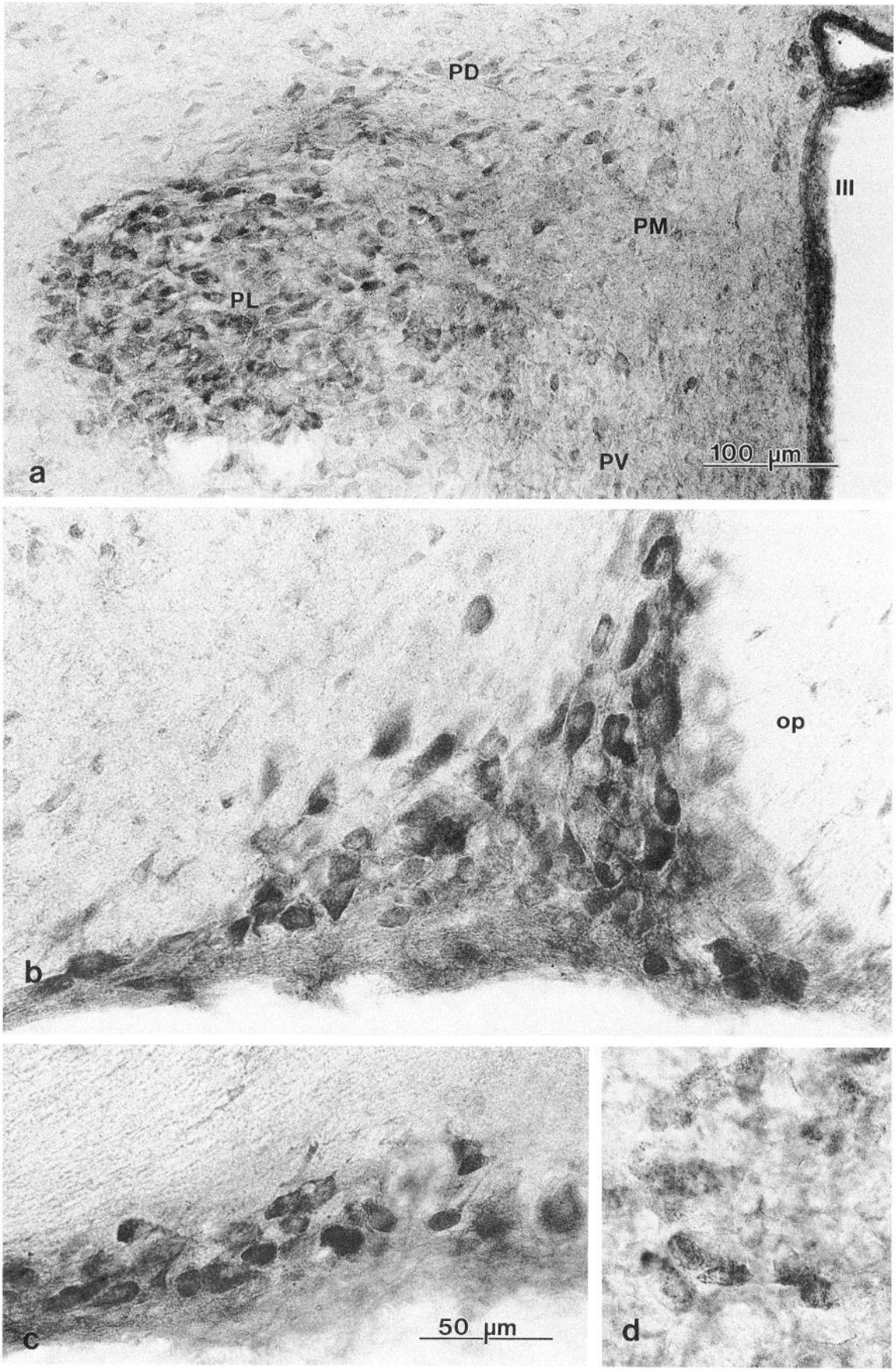

Figure 7. Hypothalamus and pituitary gland. *a,* Coronal section of the lateral magnocellular division of the paraventricular hypothalamic nucleus (*PL*). *PD, PM,* and *PV,* dorsomedial cap, medial parvocellular, and ventral divisions of the paraventricular hypothalamic nucleus; *III,* third ventricle. *b,* Sagittal section of supraoptic hypothalamic nucleus, more medial and with fewer stained, large neurons than the portion indicated in Figure 2*a*. *c,* Sagittal section of the retrochiasmatic portion of the supraoptic nucleus. *d,* Anterior lobe of pituitary gland. Magnification: *a,* 226×; *b–d,* 447×.

portion of the spinal trigeminal nucleus (Figs. 3*g*, 8*b*) can be divided into the marginal zone, gelatinous layer, and magnocellular part (Tracey, 1985). Neuropil of the marginal zone stained moderately densely and contained small to medium, and occasionally large, moderately to densely stained cells. Many of these cells were rostrocaudally elongated in sagittal sections while others were elongated parallel to the surface of the nucleus in coronal sections (Fig. 8*b*). The gelatinous layer of the caudal portion of the spinal trigeminal nucleus had a moderately to moderately densely stained, fibrous neuropil but little or no staining in cell bodies, which were obscured by the neuropilar staining. Both neuropil and the medium to large, multipolar neurons of the magnocellular part were stained lightly. In the mesencephalic trigeminal nucleus, staining was light to moderate in the neuropil and moderate to moderately dense in the large, ovoid neurons.

Auditory system. Staining was moderate to moderately dense in the ventral cochlear nucleus (Fig. 3*d*) with denser cells being more common in the posterior portion. In the dorsal cochlear nucleus (Figs. 2*b*, 3*e*), both the large fusiform neurons and the medium-sized neurons of the superficial layers were stained moderately densely to densely. In the superior olivary complex (Fig. 8*c*), neuropilar staining was generally light to moderate in the superior paraolivary nucleus, dorsal periolivary region, and nucleus of the trapezoid body, while it was moderate to moderately dense in the lateral (Fig. 8*c,d*) and medial superior olives and the latero- and medioventral periolivary nuclei. In sagittal sections, small ovoid to multipolar cells of the lateral superior olive stained moderately densely. In coronal sections, most of the stained cells were elongate ovoids oriented perpendicular to the curving long axis of the nucleus (Fig. 8*c,d*). Stained neurons were less common in the lateral limb than in the center and medial limb. Cells of most other nuclei of the complex generally stained moderately densely, while those of the medial superior olive stained moderately. The nuclei of the lateral lemniscus could be distinguished by dorsoventral columns of moderately stained neuropil, as seen in sagittal sections (PW83). In the regions between the stained columns of neuropil were rostrocaudally elongated neurons with little or no staining. The stained columns contained moderately densely stained neurons that were round to ovoid in the dorsal nucleus and ranged from multipolar to rostrocaudally elongated or rostrocaudally ovoid in the intermediate nucleus. Overall, staining in the ventral nucleus was similar to that of the dorsal nucleus but included more stained neurons and moderately to moderately densely stained patches of neuropil. In contrast to that of the nuclei of the lateral lemniscus, staining in the retrolemniscal nucleus was light to moderate only and was found in the dorsoventrally oriented processes and predominantly elongate cells. In sagittal sections (PW80–PW81), staining in the inferior colliculus (Fig. 2*a*) was most evident in the external cortex, where the small to large multipolar neurons were stained moderately to densely in a lightly stained neuropil. In more rostral portions, there were a few very large multipolar neurons that were stained lightly to moderately. In contrast, little staining was seen in the dorsal and central cortical regions of the inferior colliculus, although neuropilar staining in the dorsal cortex was slightly denser than in other regions. Light staining was seen in a few large multipolar neurons of the dorsal cortex and some small ovoid and medium multipolar cells of the central cortical region.

Vestibular system. The superior vestibular nucleus contained patches of moderately stained neuropil and moderately densely stained, medium to occasionally large neurons, which appeared multipolar in coronal sections and elongate in sagittal sections. A few of the larger neurons contained little or no staining. Neuropil of the lateral vestibular nucleus was very fibrous and punctate and was stained lightly to moderately, while staining in the many small to very large, multipolar neurons, which were often elongate–multipolar, varied from light to dense (Figs. 3*d*, 8*e*). Most of the medium, multipolar or ovoid neurons of the medial vestibular nucleus were unstained, while a few stained lightly to moderately. In contrast, the neuropil stained moderately to moderately densely. Staining of the neuropil of the spinal vestibular nucleus was moderate in the distinctive rostrocaudal patches, while staining in the small to large, multipolar to elongate neurons varied from light to dense, with most large, multipolar neurons staining lightly to moderately. Nucleus X was located just posterior to the spinal vestibular nucleus in sagittal sections (Figs. 2*a*, 8*f*; PW81), and ventrolateral to the latter in coronal sections. It contained moderately stained, ovoid to multipolar neurons in a moderately stained neuropil. Staining was very similar to that of the adjacent external cuneate nucleus (see below). Nucleus Y, located between the cochlear nuclei and the cerebellar nuclei in sagittal sections, contained very small to medium ovoid, often dorsoventrally oriented, cells that were stained moderately to densely, and a neuropil with many prominent, moderately stained processes. The prepositus hypoglossal nucleus had moderately densely stained neuropil containing a few mainly small to medium, multipolar and often elongate neurons stained lightly to moderately, although neuronal staining was somewhat obscured by neuropilar staining.

Other nuclei. Staining in most of the small neurons of the nucleus of the solitary tract was difficult to determine due to the moderately dense staining of the neuropil, although there were a few small, multipolar neurons that stained moderately. Staining of neuropil was moderate in the cuneate (Fig. 3*f,g*) and external cuneate (Fig. 2*a*) nuclei and moderately dense in the gracile nucleus (Fig. 3*f*). Stained cells seen in these structures were mainly small to medium and were stained lightly to moderately in the cuneate and external cuneate nuclei, but were obscured by neuropilar staining in the gracile nucleus and thus difficult to characterize.

Brainstem—motor

The oculomotor nucleus (Figs. 3*c*, 9*a*) contained medium to large, ovoid neurons stained moderately to moderately densely. The small to medium, dorsoventrally oriented ovoid neurons of the Edinger-Westphal nucleus (Fig. 9*a,b*) were stained similarly. Many of these neurons showed a pronounced preferential staining on one side of the soma. Neuropil staining was moderate in the former and light in the latter nucleus. Neuropil was light in the abducens nucleus, which contained large, moderate to moderately densely stained multipolar neurons. The large multipolar neurons of the trigeminal motor nucleus were among the densest stained cells in the lower brainstem (Figs. 2*a*, 9*c*). A few smaller multipolar cells stained lightly to moderately. Staining of the neurons of the facial motor nucleus (Figs. 2*a*, 9*d,e*), including medium to large multipolar and dorsoventrally elongated multipolar neurons, was moderately dense to dense, while the neuropil stained moderately with numerous puncta. More cells with dense staining were seen in the lateral (coronal sections) and caudal (sagittal sections) portions of this nucleus, including some small to medium dorsoventrally elongate cells in the latter. The nucleus ambiguus (Fig. 9*d,f*) contained patch-

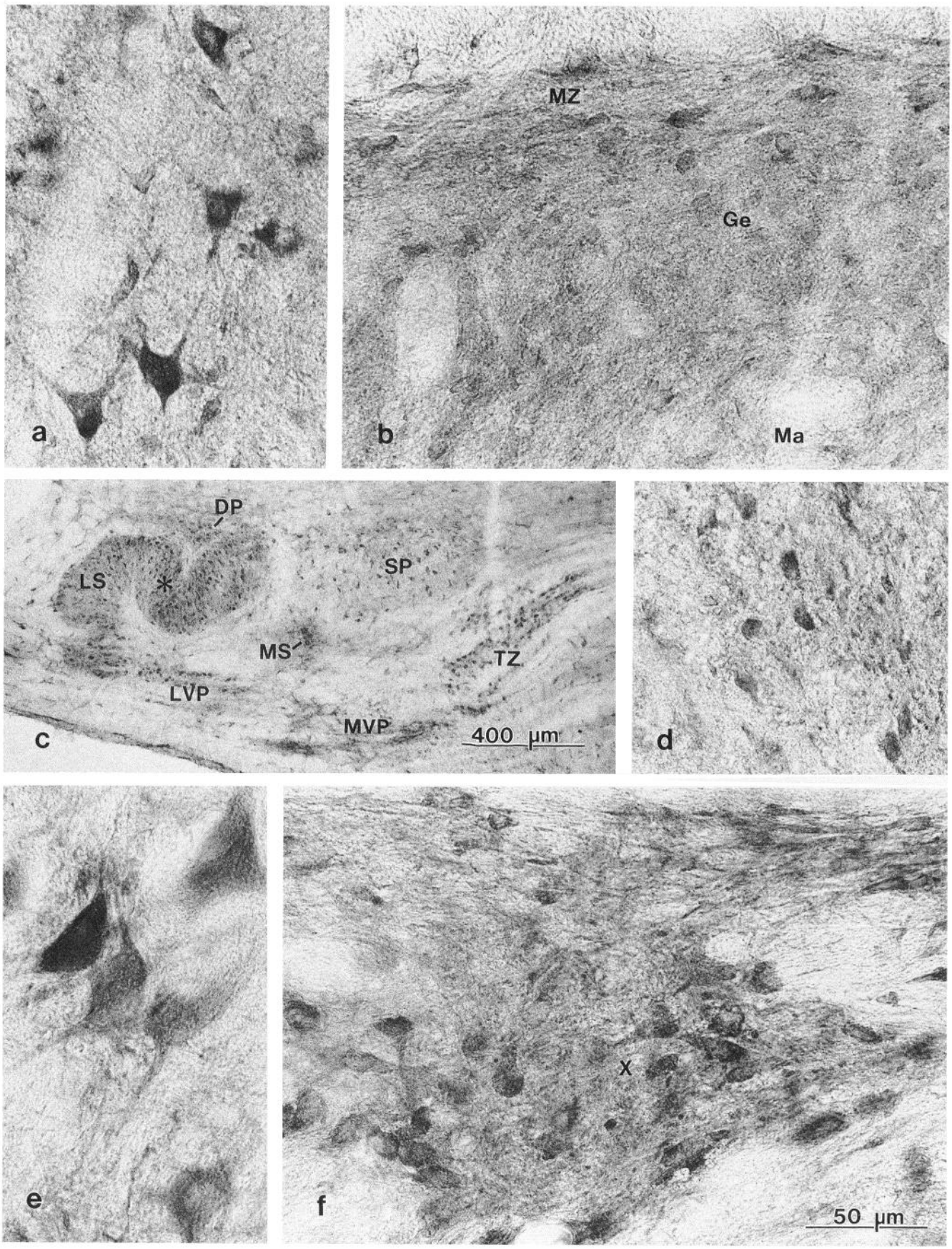
a
b
MZ
Ge
Ma
c
DP
LS
*
SP
MS
TZ
LVP
MVP
400 µm
d
e
f
X
50 µm

es of moderately densely stained neuropil, densely stained, medium to large multipolar neurons of various types, and some lightly to moderately stained multipolar neurons. Staining in the dorsal motor nucleus of the vagus nerve was moderate both in neuropil and in the medium, mediolaterally elongate to ovoid neurons. Neuropilar staining in the hypoglossal nucleus (Fig. 3*f*) was moderate to moderately dense with many puncta. The large multipolar neurons stained moderately densely and were more common in the ventral portion. Neurons of the supraspinal nucleus were identified in the ventromedial portion of the ventral horn at the spinomedullary transition area, which was identified by the presence of the corticospinal decussation and dorsal column nuclei (Carpenter and Sutin, 1983). The supraspinal nucleus contained a number of small to large, densely stained multipolar neurons as well as a few large, lightly stained multipolar ones.

Brainstem—reticular core and central gray

Most areas of the reticular core and central gray contained moderately stained neurons in a neuropil ranging from unstained to moderately stained. Notable exceptions included the inferior olive (Fig. 3*f*) and lateral reticular nucleus (Figs. 2*a*, 3*f*). Staining of the neuropil in most examined regions of the inferior olive was moderate to moderately dense, while that of the cap kooy medial nucleus was light to moderate. Stained neurons of the inferior olive were mainly medium multipolar, and most were stained moderately densely. In coronal sections, many of the medium to large, stained neurons of the lateral reticular nucleus were stained moderately densely, and neuropilar staining was moderate. In sagittal sections, the lateral reticular nucleus contained rostrocaudally oriented bands of neuropil stained moderately to moderately densely with little or no staining between them. Neurons in these bands also were oriented rostrocaudally. They were ovoid to elongate and ranged from small to large, with the densest staining seen in small to medium, elongate cells. The unstained areas between the bands of dense neuropil contained lightly stained, large, dorsoventrally oriented neurons. In contrast to the lateral reticular nucleus, there was little or no staining in the parvocellular portion of the lateral reticular nucleus, and the small, multipolar neurons stained moderately. Neuropilar staining in the red nucleus (Figs. 3*c*, 10*a*) was light in the parvocellular portion and moderate in the magnocellular portion. Both portions contained medium, multipolar neurons that stained moderately to moderately densely. In addition, the magnocellular portion contained large, moderately stained neurons. In the pontine nuclei (Figs. 2*a*, 10*b*), staining was moderately dense in the fibrous neuropil and moderate to dense in the small to medium cells. The latter were collected in bundles, as well as being interspersed among the unstained nerve fiber bundles.

Cerebellum

Staining in most portions of the cerebellar nuclei (Fig. 2) was light to moderate in both neuropil and the mainly multipolar neurons. Densest staining was seen in the dorsal region of the lateral cerebellar nucleus (coronal sections) and portions of the interposed and medial cerebellar nuclei.

The most prominent staining in the cerebellar cortex (Figs. 2, 3, 10*c*) was in the Purkinje cells, which had densely stained cell bodies and moderately densely stained dendritic arbors. Golgi cells of the granular layer stained lightly to moderately, while staining was light in the small cells of the molecular layer. Overall staining in the granular layer was light to moderate, and that of the molecular layer was moderate. Some variation was seen in staining, especially of Purkinje cell bodies, along the extent of the cerebellar cortex, although a specific pattern was not obvious. Probably, at least part of this can be attributed to artifacts in the preparation (Fig. 2).

Fibers of the three cerebellar peduncles and cerebellar cortical white matter appeared to be unstained. However, in the cortical white matter and middle and superior peduncles, as in most areas of white matter in the brain, staining of glia ranged from very light to light, while glia of the inferior peduncle were stained slightly denser.

Cervical spinal cord

Coronal sections from the middle segments of the cervical spinal cord (Figs. 3*h*, 10*d*) contained moderately densely stained neuropil in laminae I–III and X and moderately dense to dense staining in the large motoneurons of lamina IX. Moderately stained neurons were seen in all laminae, although stained neurons were absent from the inner portion of lamina II and were uncommon in lamina X. Moderately densely stained neurons were seen in all laminae but were uncommon except for small, horizontally elongate neurons of lamina I.

Electron microscopy—controls

Control sections in which PBS was substituted for the primary antibody were examined with electron microscopy. All layers in each of the cerebral cortex (Fig. 11*a*), hippocampus (Fig. 12*a*), and cerebellar cortex (Fig. 13*b*) were studied. In the cerebral cortex and hippocampus, light staining was seen occasionally in numerous vesicles enclosed in a large, membrane-bound organelle that also contained unidentifiable, fibrous matrix material (Fig. 11*a*). Presumably, these are types of multivesicular bodies, based on the broad definition (Peters et al., 1991), but may be different from the more definitive type, which contains mainly vesicles, and which were never seen to be stained in control sections. Otherwise, in all three brain regions, staining was absent from all cytoplasmic structures, while myelin staining was mostly moderate, but varied from light to dense (Fig. 11*a*). Postsynaptic densities were never stained in the cerebral cortex (Fig. 11*a*), mossy terminals of CA3 of the hippocampus (Fig. 12*a*), or cerebellar cortex (Fig. 13*b*). However, the stratum oriens and molecular layer of CA3 and CA1/CA2 (i.e., border region between CA1 and CA2) contained rare, small spines with lightly stained postsynaptic densities. In addition, in the proximal region of the molecular layer of CA1/CA2, we found one

←

Figure 8. Neurons of sensory nuclei. *a,* Sagittal section of area of large neurons associated with the deep gray layer of the superior colliculus. *b,* Coronal section from caudal brainstem, showing the caudal portion of the spinal trigeminal nucleus. *MZ*, marginal zone with some moderately stained elongate neurons; *Ge*, gelatinous layer, showing mostly ovoid cell profiles with little or no staining; *Ma*, edge of magnocellular part. *c,* Coronal section of superior olivary complex. *DP*, dorsal periolivary region; *MS* and *LS*, medial and lateral superior olives; *LVP* and *MVP*, lateroventral and medioventral periolivary n.; *SP*, superior paraolivary n.; *TZ*, trapezoid body. *Asterisk*, portion of middle superior olive shown in high magnification in *d. e,* Sagittal section of lateral vestibular nucleus showing one densely and four moderately stained, large neurons. *f,* Sagittal section of nucleus X (*X*; location shown in Fig. 2*a*). Magnification: *a, b,* and *d–f,* 447×; *c,* 56×.

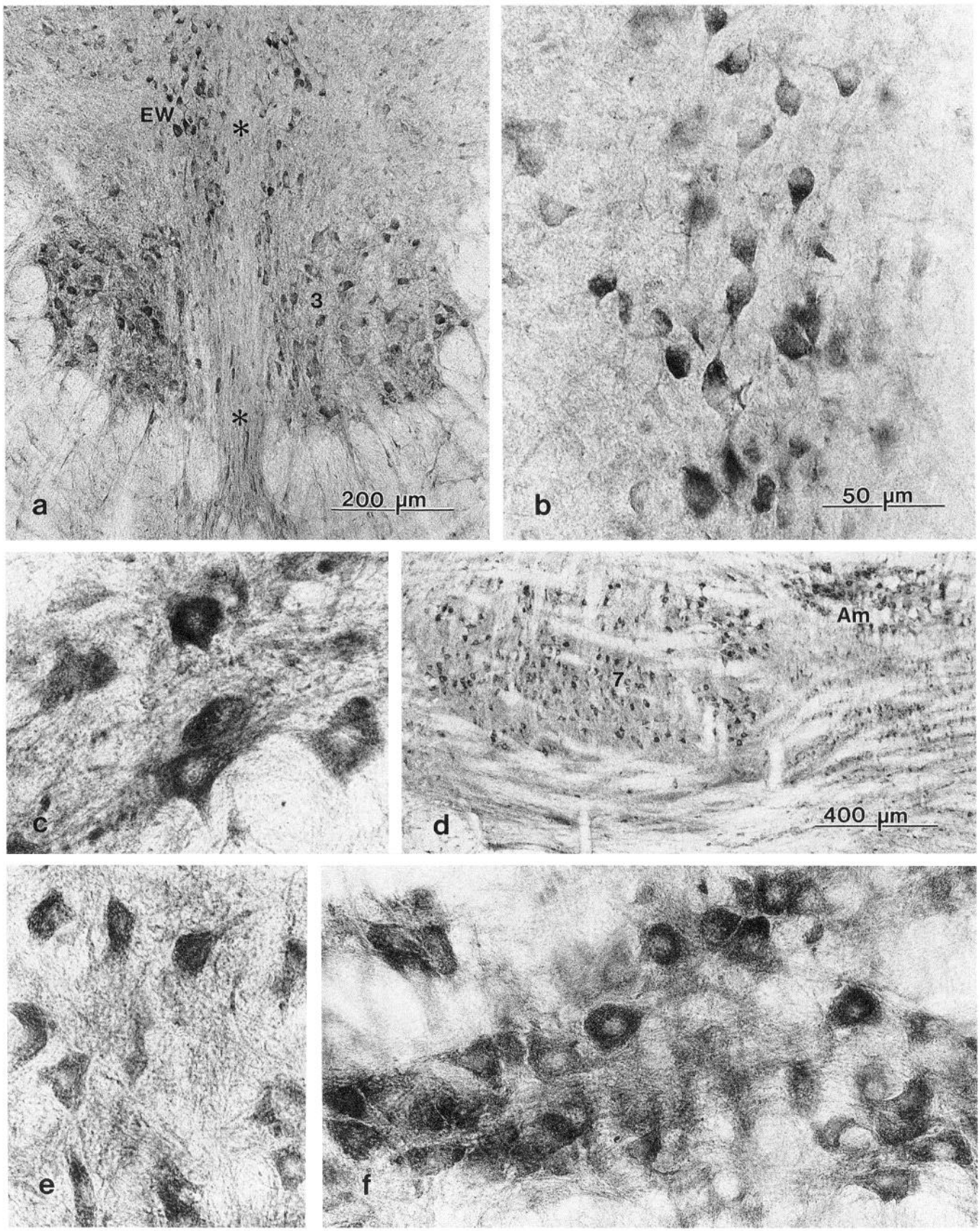

Figure 9. Neurons of motor nuclei. *a,* Coronal section of oculomotor (*3*) and Edinger-Westphal nucleus (*EW*). *Asterisks,* midline. *b,* High magnification of Edinger-Westphal nucleus. *c,* Sagittal section of motor trigeminal n. *d,* Sagittal section of facial (*7*) and ambiguus (*Am*) nuclei, shown in high magnification in *e* and *f,* respectively. Magnification: *a,* 112×, *b, c, e,* and *f,* 447×; *d,* 56×.

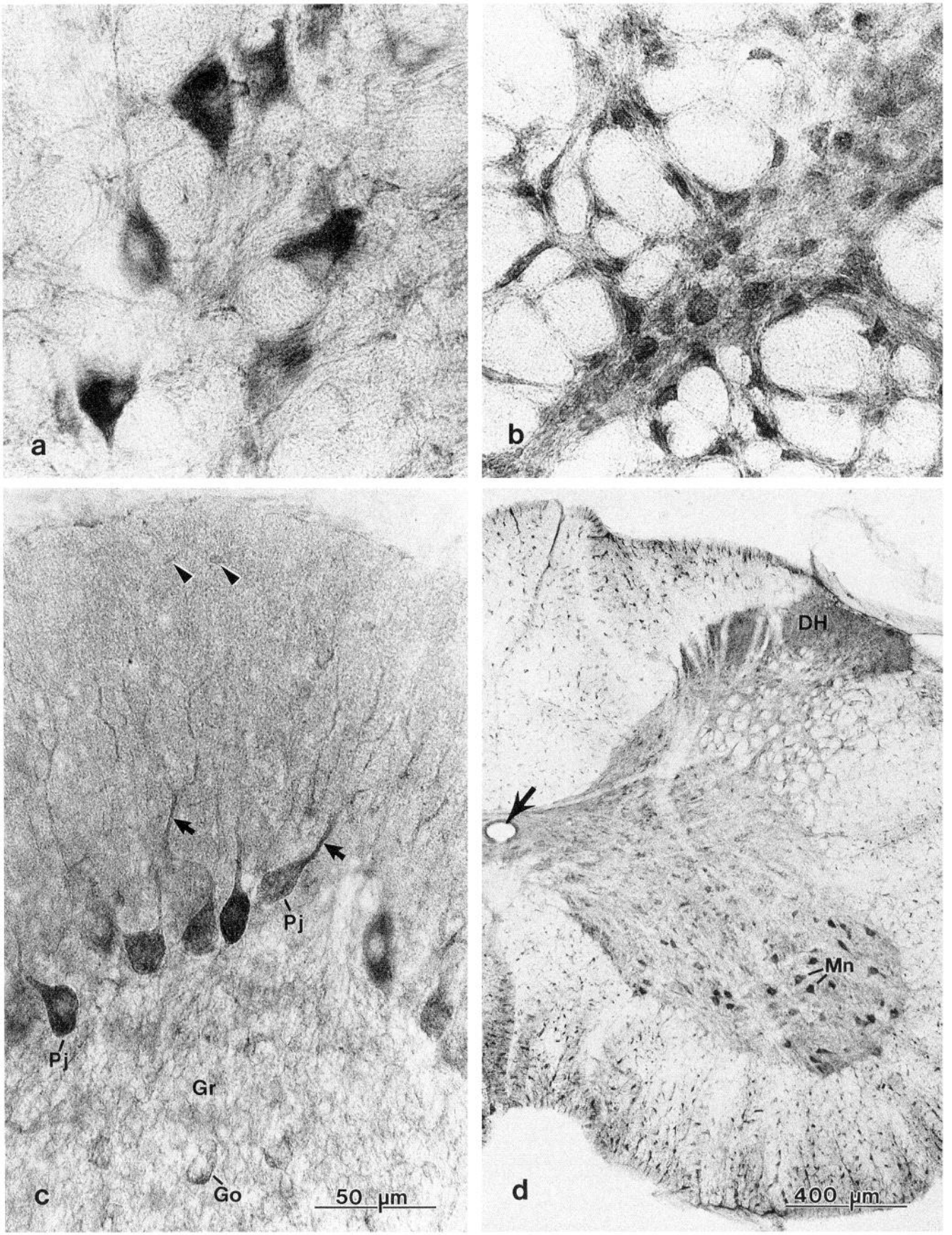

Figure 10. Reticular nuclei, cerebellar cortex, and cervical spinal cord. *a,* Coronal section of red nucleus. *b,* Sagittal section of pontine nuclei. *c,* Sagittal section of cerebellar cortex. *Gr*, granular layer; *Go*, Golgi cell; *Pj*, Purkinje cell. *Arrows*, Purkinje cell dendrites; *arrowheads*, molecular layer cells. *d,* Transverse section of cervical spinal cord. *DH*, outer dorsal horn (laminae I–III); *Mn*, motoneurons of ventral horn (lamina IX). *Arrow*, central canal (surrounded by lamina X). Magnification: *a–c,* 447×; *d,* 56×.

example of a small spine synapse with a postsynaptic density with staining within the range seen in synapses immunolabeled definitively with antibody to NMDAR1.

Electron microscopy—general

In all regions studied (Figs. 11–13), cerebral cortex, hippocampus, and cerebellar cortex, immunostaining was found in neuron cell bodies and dendrites and in the postsynaptic densities of synapses. Staining was not seen in the synaptic cleft, while staining in presynaptic terminals was rare and not definitive, as described for AMPA receptors in the brain (Petralia and Wenthold, 1992; see also Molnár et al., 1993). Staining in cytoplasm of dendrites was concentrated in patches associated with groups of microtubules and/or the surface of one pole of a mitochondrion. Patches of staining in the cell body formed similar associations, as well as being associated with rough endoplasmic reticulum, Golgi apparatus, and the nuclear envelope. In the cerebral cortex, an occasional, stained multivesicular body bearing a fibrous matrix, as defined for the description of control sections, was found in neuron cell bodies, and contained densely stained vesicles. In contrast, in all brain regions, staining was not observed in multivesicular bodies that lacked a fibrous matrix. Sections from all regions included some stained processes that could not be identified. Many of these presented narrow profiles with few cytoplasmic structures and could be dendritic spines and/or glial processes as discussed for AMPA receptors (Petralia and Wenthold, 1992). However, staining was not seen in definitive glial cells.

Electron microscopy—cerebral cortex

Specific layers could not be delineated easily in thin sections, although stained dendrites and postsynaptic densities were seen throughout the dorsoventral extent of the gray matter. The densest stained synapses were asymmetric type I and were composed of a postsynaptic dendritic spine bearing a densely stained postsynaptic density apposed to an unstained presynaptic terminal filled with round or pleomorphic (mostly round) vesicles (Fig. 11*b–d*). In addition, a few stained postsynaptic densities were on the shafts of small dendrites and these were apposed to unstained presynaptic terminals. Overall, immunostaining of postsynaptic densities ranged from densely stained to unstained, with many synapses showing moderate levels of staining (Fig. 11*b,c*).

Electron microscopy—hippocampus

In the stratum oriens of CA3 (Fig. 12*d*) and CA1/CA2 (Fig. 12*e*) regions as well as the molecular layer of these regions, the most common immunostained synapses (type I with asymmetric densities) had postsynaptic spines bearing densely stained postsynaptic densities apposed to unstained presynaptic terminals containing round or pleomorphic (mostly round) vesicles. In addition, in the region of the proximal portions of the apical dendrites of the CA3 pyramidal cells, moderate staining was seen in some postsynaptic densities apposed to unstained mossy fiber terminals (Fig. 12*b,c*). These stained postsynaptic densities were part of active zones of the specialized dendritic spines of the apical pyramidal cell dendrites. However, most postsynaptic densities apposed to mossy fiber terminals contained little or no definitive staining. In addition, a few stained postsynaptic densities were seen on the shafts of these dendrites, apposed to similar presynaptic mossy fiber terminals, as mentioned for AMPA receptors (Petralia and Wenthold, 1992). Some patches of stain were seen in thin, presumptive unmyelinated axons found in bundles in the mossy fiber terminal region (Fig. 12*b*) and may be the mossy fibers (Blackstad and Kjaerstad, 1961) or fibers associated with them. No definitive examples of stained presynaptic terminals were seen.

Electron microscopy—cerebellar cortex

Staining in the granular layer was found mainly in a few scattered processes, most of which appeared to be small dendrites. Definitive staining of synapses was not seen in the granular layer. Most granule cell bodies appeared unstained or contained only a few small patches of stain. However, substantial staining was seen in some small to medium cells in all layers. Staining in Purkinje cell bodies consisted of numerous patches of staining associated with organelles (Fig. 13*a*), including rough endoplasmic reticulum, Golgi apparatus, and mitochondria. Occasional staining was associated with the cell membrane apposed to possible, unstained presynaptic terminals but these were not definitive. The molecular layer contained numerous, small, stained processes, most of which appeared to be small dendrites, as well as the large, stained dendrites of the Purkinje cells. Synapses with stained postsynaptic densities were seen throughout the molecular layer. These were asymmetric, type I, with the postsynaptic dendritic shaft or dendritic spines containing stained postsynaptic densities, apposed to unstained presynaptic terminals with round or pleomorphic (mostly round) vesicles. Most of the synapses consisted of single, unstained, presynaptic terminals apposed to single postsynaptic spines, usually with the stained active zone on the side of the spine head, and ensheathed by possible glial processes. In some cases, the spine could be traced to putative spiny branchlets of Purkinje cell dendrites (Fig. 13*c,d*). Thus, they matched previous descriptions of parallel fiber–Purkinje spine synapses (Mugnaini, 1972; Palay and Chan-Palay, 1974), although the majority of parallel fiber–spine synapses seen in sections were unstained (Fig. 13*d*). Often, the spine projected into the center of the presynaptic terminal, and many synapses contained a densely stained structure in the spine, just below the stained postsynaptic density (Fig. 13*c,d*). Synapses with stained postsynaptic densities on small-caliber dendritic shafts were uncommon, as were synapses with stained postsynaptic densities apposed to terminals with pleomorphic, but mostly ovoid, vesicles. No definitive example was seen of staining associated with climbing fiber synapses, that is, with many, densely packed, large, round vesicles surrounded by a dark, filamentous matrix in the presynaptic terminal, apposed to short spines on the main dendritic shafts of Purkinje cells (Palay and Chan-Palay, 1974). Also, staining was seen in some of the processes similar to and interspersed with parallel fibers. Occasionally, unidentified stained processes were associated with unstained or lightly stained synapses. The former resembled glial processes, although distinct labeling of glia was not seen.

Discussion

The present data suggest that the NMDA receptor subunit NMDAR1 is widespread throughout the CNS and exists in some neuron populations in most major nuclear groups, as well as in some glia, sensory ganglion cells, and endocrine organs. Electron microscope studies of hippocampus, cerebral cortex, and cerebellar cortex have indicated that this subunit is present in postsynaptic densities of synapses, and is associated with cytoplasmic structures in a pattern that is consistent with the synthesis, processing, and transport of this protein, as described for AMPA

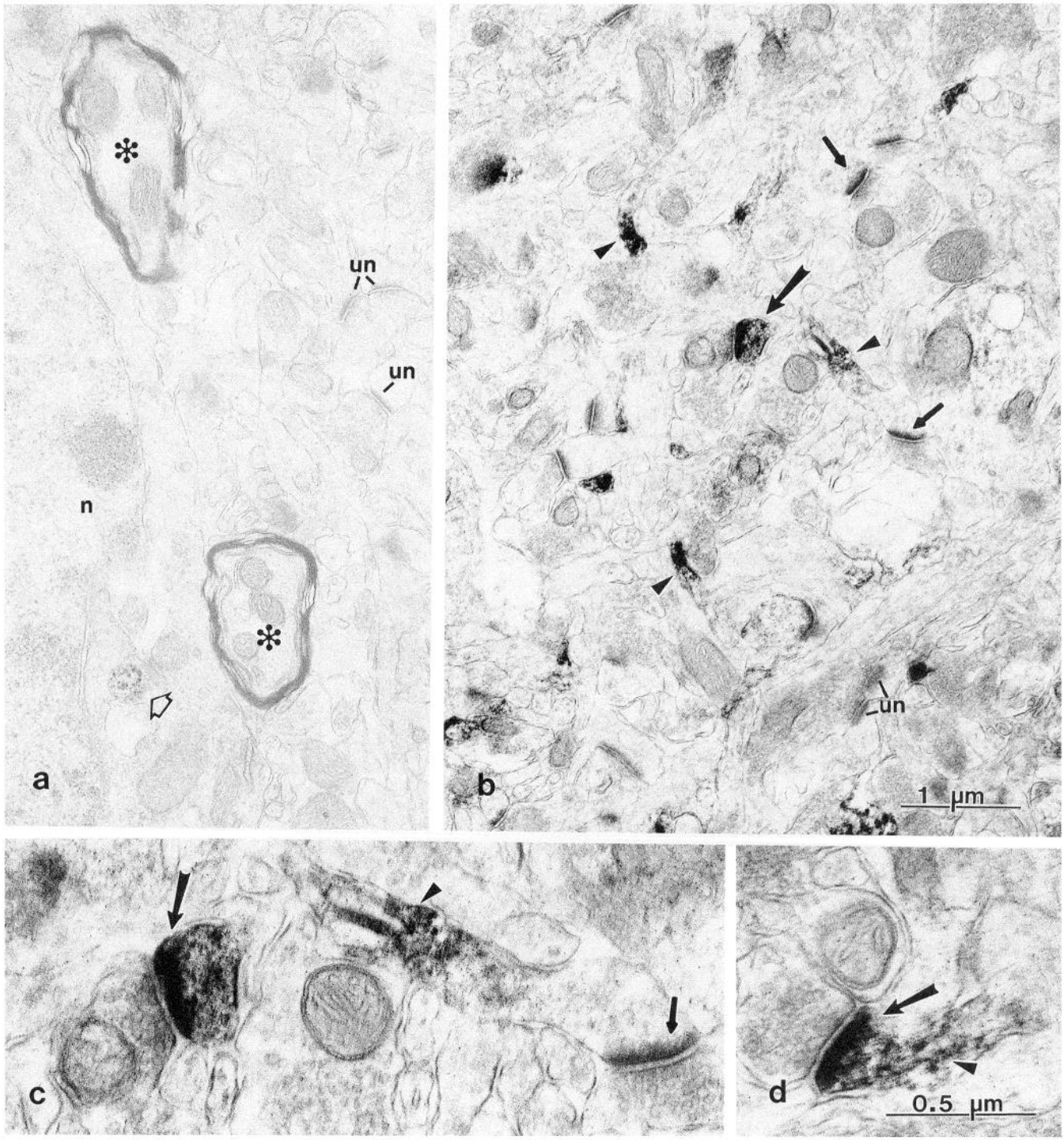

Figure 11. Electron micrographs of cerebral cortex. Immunostaining with antibody to NMDAR1 is shown in *b–d.* All were taken from the outer layers of the cortex. *a,* Control section (no primary antibody) shows complete absence of immunostaining in cytoplasm, nucleus (*n*), myelinated axons (*asterisks*), and postsynaptic densities (*un*). Note the light staining in a type of multivesicular body (*open arrow*) in cell body cytoplasm. *b,* Low magnification shows dense staining in a postsynaptic density (*large arrow*) in a dendritic spine, and in dendritic processes (*arrowheads*). Staining of postsynaptic densities varies from dense to moderate (*small arrows*) to those with little or no specific staining (*un*). *c,* High magnification of synapses in center of *b*. Note immunostaining (*arrowhead*) in the lower portion of the spine neck of the synapse on the right. *d,* Example of a synapse with a densely stained postsynaptic density (*arrow*) and staining in the neck of the dendritic spine (*arrowhead*). Magnification: *a* and *b,* 20,000×; *c* and *d,* 50,000×.

receptor subunits (Petralia and Wenthold, 1992; Martin et al., 1993). Many cells throughout the nervous system stained densely for NMDAR1, and it is likely that NMDA receptors are one of the major glutamate receptor types in these cells. However, the significance of the light to moderate staining seen in many other cells and often characterizing entire nuclei is not clear. We cannot rule out the possibility that the lighter staining (e.g., less than 2 in the Appendix) represents a nonspecific background staining. Alternatively, NMDAR1 (i.e., the four splice variants recognized by our antibody) may be present in only a limited

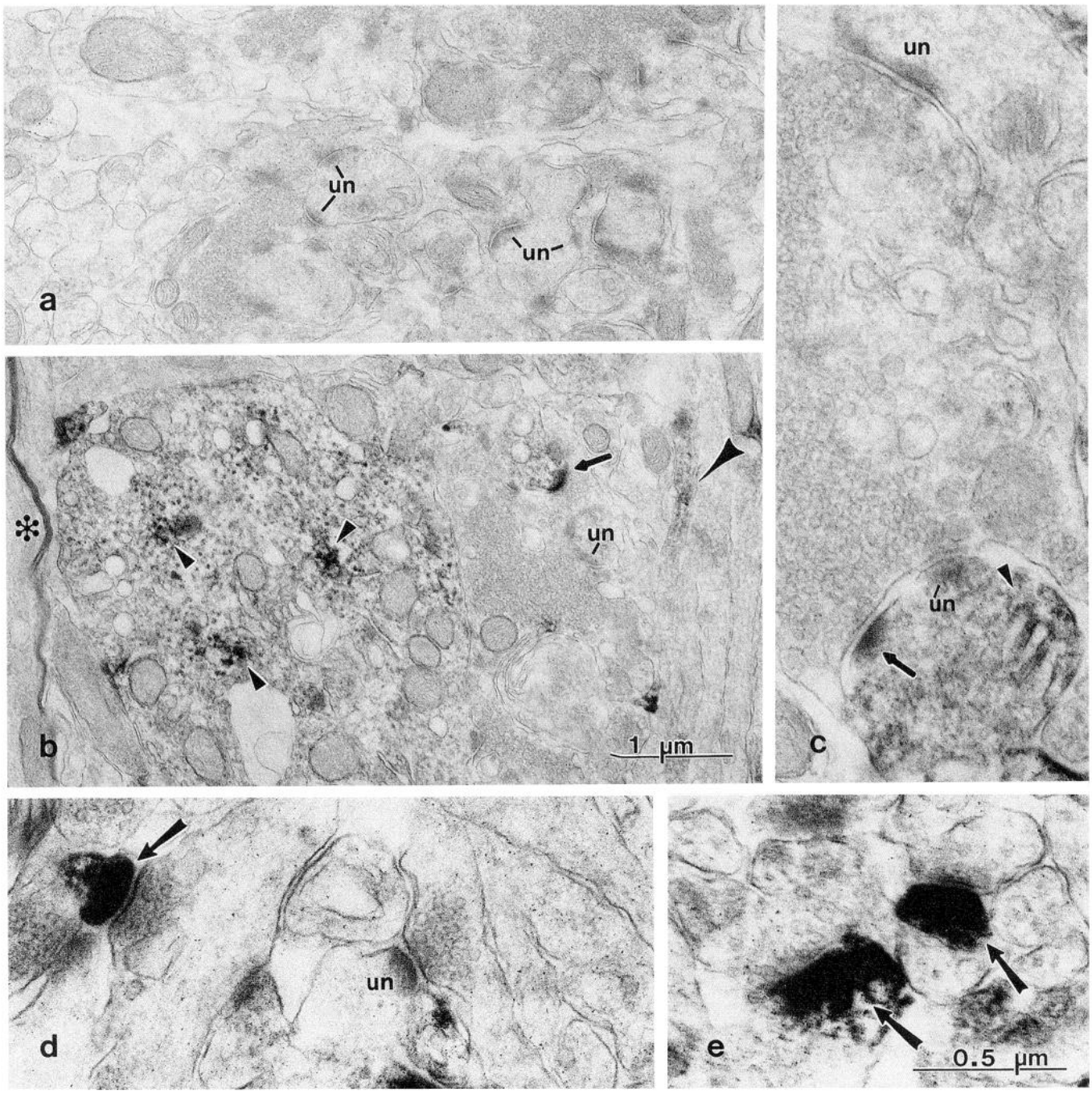

Figure 12. Electron micrographs of hippocampus. Immunostaining with antibody to NMDAR1 shown in *b–e*. *a*, Control section (no primary antibody) shows complete absence of immunostaining (*un*) in postsynaptic densities of mossy fiber synapses on specialized spines of apical dendrites of pyramidal cells of the CA3 region. *b*, Presumed apical dendrite of pyramidal cell of CA3 region with patches of immunostaining (*small arrowheads*). Most postsynaptic densities of mossy fiber synapses are unstained (*un*), but a few are stained moderately (*arrow*). *Asterisk*, Unstained myelinated fiber; *large arrowhead*, staining in a process that is part of a group of presumptive, unmyelinated axons. *c*, High magnification of mossy fiber terminal synapses of specialized spines of apical dendrites of pyramidal cells of CA3 region. Most postsynaptic densities are unstained (*un*) while some show light to moderate staining (*arrow*). *Arrowhead*, staining in spine. *d* and *e*, Dense staining in postsynaptic densities (*arrows*) in dendritic spines in the stratum oriens of CA3 (*d*) and CA1/CA2 (*e*) regions. *un*, postsynaptic density with little or no staining. Magnification: *a* and *b*, 20,000×; *c–e*, 50,000×.

→

Figure 13. Electron micrographs of cerebellar cortex. Immunostaining with antibody to NMDAR1 shown in *a*, *c*, and *d*. *a*, Purkinje cell body showing patches of immunostaining (*arrowheads*) in the cytoplasm. *n*, nucleus. *b*, Control section from upper molecular layer (no primary antibody) shows complete absence of immunostaining in cytoplasm and postsynaptic densities (*un*). *c*, Immunostained postsynaptic density (*arrow*) on side of head of spine attached to a Purkinje cell spiny branchlet (*sb*). *t*, parallel fiber terminal. Note dense structures (*arrowhead*) just below postsynaptic density. *d*, Same type of immunostained parallel fiber–Purkinje spine synapse as in *c*. However, the attachment of the spine to the spiny branchlet is not as distinct. Adjacent to this is a similar, but unstained (*un*), parallel fiber–spine synapse. Magnification: *a*, 20,000×; *b–d*, 50,000×.

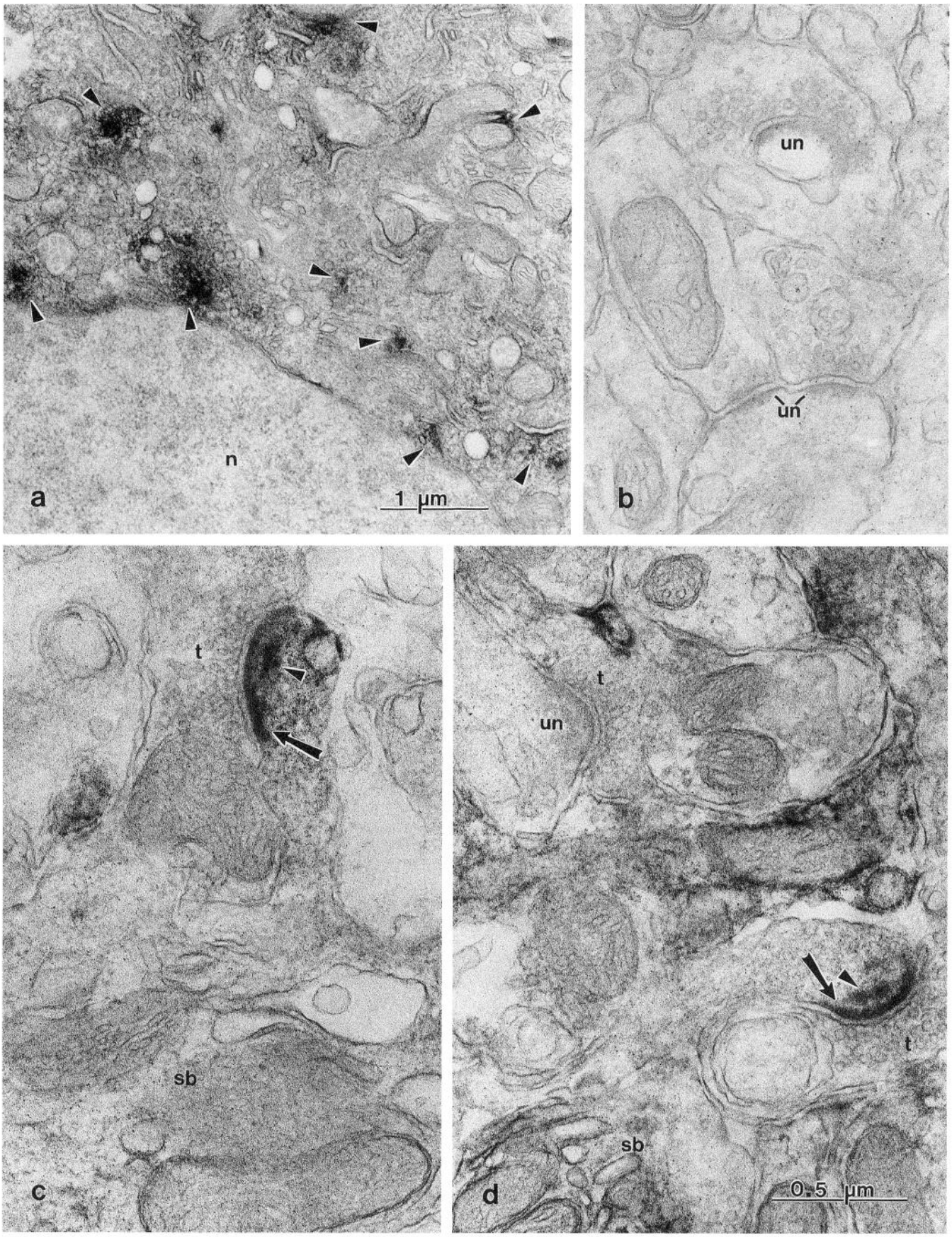
a
n
1 µm
b
un
un
c
t
sb
d
t
un
t
sb
0.5 µm

number of synapses on these neurons, or may be present in many synapses but at low levels. These possibilities are supported by our electron microscope findings, which suggested that in some cases, NMDAR1, associated with certain cell types, is present in discrete subpopulations of synapses and/or is expressed in synapses at low levels.

Comparison to in situ *hybridization and ligand binding studies*

The widespread expression of NMDAR1 protein seen in our study matches closely with the equally widespread distribution of mRNA for NMDAR1, as shown with RNA blot analysis and *in situ* hybridization (Moriyoshi et al., 1991). This study showed densest bands of RNA in the hippocampus, hypothalamus, and olfactory bulb, as well as substantial RNA in the cerebral cortex, cerebellum, midbrain, striatum, medulla/pons, and spinal cord. One of the figures in this study is a horizontal section of the brain (Fig. 5*a* of Moriyoshi et al., 1991) that shows high levels of hybridization in the olfactory bulb, cerebral cortex, hippocampus, entorhinal and subicular regions, and cerebellum, with substantial levels in striatum, thalamus, lateral septum, colliculi, and cerebellar nuclei. While the description of anatomical distribution in this latter study was not comprehensive, it seems apparent that most of the staining that was evident in our immunocytochemical study can be matched to the distribution of mRNA for NMDAR1. In the hippocampus, these authors found that all major groups of neurons had high levels of hybridization, including the CA1–CA3 pyramidal cells, and neurons of the hilus and granular layer of the dentate gyrus. This matches our findings of high levels of staining in both the cell bodies and dendrites of neurons of the CA1–CA3 region and the hilus. In addition, the high levels of RNA for NMDAR1 seen in the granule cells of the dentate gyrus may correspond to the substantial antibody staining that we saw at the boundary of granular and molecular layers and in the proximal third of the molecular layer, that is, the region of the proximal portions of granule cell dendrites. One slight difference between our study and the RNA study of Moriyoshi et al. (1991) may be in expression levels in the cerebellar cortex. These authors report highest hybridization in the granular layer (supported by binding studies, e.g., Monaghan and Cotman, 1985; Jansen et al., 1990), although their figure (Fig. 5*c* of Moriyoshi et al., 1991) appears to reveal substantial levels in Purkinje cells and cells of the molecular layer, as well as in Golgi and granule cells of the granular layer (see also N. Nakanishi et al., 1992). In comparison, we found the greatest amount of immunostaining in the Purkinje cells, although we did find substantial staining overall in both molecular and granular layers, including Golgi cells of the granular layer and, to a lesser extent, cells of the molecular layer. One explanation for our finding of the greatest amount of staining in the Purkinje cells and only moderate staining in the granular layer may be that our C-terminus antibody recognizes only some of the splice variants of NMDAR1; that is, our antibody recognizes only four of the seven splice variants known (Sugihara et al., 1992). Also, this could explain why we found only light staining for NMDAR1 in the immunoblot analysis of the cerebellum, compared to the high overall expression of NMDAR1 RNA in the cerebellum indicated by blot analysis (Moriyoshi et al., 1991).

While results of *in situ* hybridization studies are very similar to our immunocytochemical results, comparison of our data to those of ligand binding studies reveals many discrepancies. A number of different NMDA ligand-binding sites, including NMDA-sensitive L-^{3}H-glutamate (Monaghan and Cotman, 1985), ^{3}H-glutamate–sensitive NMDA, and ^{3}H-*N*-(1-[2-thienyl]cyclohexyl)3,4-piperidine–labeled phencyclidine (TCP-PCP; Maragos et al., 1988), ^{3}H-3-((+)-2-carboxypiperazin-4-yl)propyl-1-phosphonic acid (CPP; Kito et al., 1990), and ^{3}H-(+)-5-methyl-10,11-dihydro-5H-dibenzo[a,d]cyclohepten-5,10-imine (^{3}H-MK-801; Subramaniam and McGonigle, 1991), have been utilized to determine NMDA receptor distribution in the rat brain. Results of these studies have suggested that NMDA receptors are widespread in the CNS, in line with our data. These binding studies tended to show moderately high to high levels in certain forebrain regions, including parts of the hippocampus, cortex, thalamus, and olfactory structures, as in our immunocytochemical studies. However, the former studies showed low to moderate levels in the hypothalamus, midbrain, hindbrain, and spinal cord. Thus, they do not support our findings, which indicate relatively high levels of NMDAR1 in many structures in these regions, for example, supraoptic hypothalamic nucleus, Purkinje cells of the cerebellum, and some neurons in certain brainstem sensory, motor, and reticular nuclei. In addition, ligand binding often was higher in dendritic regions than in cell body regions. In comparison, we found that many major structures had substantial immunoreactivity in cell bodies, for example, the hippocampal pyramidal cells and cerebellar Purkinje cells. Probably, this reflects the presence of a substantial cytoplasmic pool of NMDAR1 molecules, as discussed for AMPA receptors (Petralia and Wenthold, 1992). Thus, one explanation for the high levels of immunoreactivity that we see in many structures, which contain low levels of ligand binding, is the presence of many receptor polypeptides in the cytoplasm of cells that bear few receptor molecules on their plasma membrane, that is, those receptor molecules exposed to extracellular ligands and presumably identified in ligand binding studies.

Alternatively, or in addition, it is likely that many of the discrepancies in NMDA receptor distribution, seen when comparing ligand binding studies to either our immunocytochemical data or to previous *in situ* hybridization studies (discussed in Moriyoshi et al., 1991), are due to the presence of multiple receptor subtypes. Results from ligand binding studies have indicated that there are many subtypes of NMDA receptors (review by Monaghan, 1991). For example, the ability of different competitive NMDA receptor antagonists to inhibit L-^{3}H-glutamate or ^{3}H-MK-801 binding differs in the forebrain, cerebellum, and medial regions of the thalamus, indicating that there are at least three pharmacologically distinct types with different anatomical distributions (Beaton et al., 1992). Sakurai et al. (1993) examined regional differences in regulation of ^{3}H-MK-801 binding in the forebrain of the rat, and found changes in the anatomical distributions of ^{3}H-MK-801 binding depending on the antagonist used, implying that there may be two or more subtypes expressed in different proportions within a region. Undoubtedly, at least some of the diversity of NMDA receptor subtypes, as suggested by these binding studies, is due to the presence of heteromeric assemblages of the various NMDA subunits (Sakurai et al., 1993), most likely involving NMDAR1 subunits in combination with one or more kinds of the NMDAR2 subunits (Monyer et al., 1992; reviewed by Nakanishi, 1992). Thus, different anatomical regions may contain NMDA receptors with different heteromeric compositions, since they express different combinations of the subunits. For example, while all areas of the brain have substantial levels of the R1 subunit, they

contain only some of the R2 subunits, that is, R2A and R2C in the cerebellum, R2A and R2B in the amygdala and caudate-putamen, R2A and R2B in the granule cells of the olfactory bulb, R2A and R2C in the mitral and tufted cells of the olfactory bulb, R2A-C in the thalamic nuclei, and none of these three R2 subunits in the hypothalamus (Monyer et al., 1992). In addition, the R2D subunit seems to be the major R2 subunit in the lower brainstem as well as being one of the subunits found in the diencephalon (Nakanishi, 1992). Similar results have been found in the mouse brain with the equivalent R2A–R2C subunits of the mouse, that is, $\epsilon 1$–$\epsilon 3$ (Kutsuwada et al., 1992; Meguro et al., 1992). Also, splice variants of NMDAR1 may be differentially distributed, since in most parts of the brain, the major form, NMDAR1A, may be five times more abundant than NMDAR1B, but this ratio is reversed in the cerebellum, where there appears to be five times more R1B (N. Nakanishi et al., 1992).

NMDA receptors in the cerebral cortex

Immunostaining for antibody to NMDAR1 was moderate in most regions of the iso- and allocortex, with staining localized preferentially to pyramidal cells. Stained postsynaptic densities apposed by unstained presynaptic terminals appeared to be present throughout the layers of the cortex. Presence of NMDA receptors in the cerebral cortex is supported by a large body of evidence from binding (see above), pharmacological, and electrophysiological studies (e.g., Brooks et al., 1991; Cox et al., 1992; reviewed by Stone and Burton, 1988). No definitive evidence of presynaptic immunostaining was seen, although the presence of NMDA receptors on presynaptic noradrenergic varicosities in the cortex has been suggested (Fink et al., 1990, 1992; Wang et al., 1992). One of the most interesting findings was the distinctive staining of putative rat barrel fields in the parietal cortex, area 1. Our staining corresponds closely with the distribution of NMDA binding sites in barrel fields, as labeled with the competitive antagonist ^{3}H-CGP39653 or with ^{3}H-glycine in the presence of strychnine (Jaarsma et al., 1991). These authors found only homogeneous binding of ^{3}H-AMPA in this region, and concluded that the distribution of NMDA, but not AMPA, receptors may correspond to the zone of termination of specific sensory afferents from the ventral posterior nucleus of the dorsal thalamus (see also Armstrong-James et al., 1993). Similarly, we found only homogeneous immunostaining with an antibody to the AMPA receptor subunit GluR1, although barrel fields are stained distinctively with an antibody that recognizes the kainate receptor subunit GluR6 (and recognizes GluR7 to a lesser extent; Wenthold et al., in press; R. S. Petralia, Y.-X. Wang, and R. J. Wenthold, unpublished observations), indicating a possible colocalization of NMDA and kainate receptors in rat barrel fields.

NMDA receptors in the hippocampus

Substantial immunostaining with antibody to NMDAR1 was seen throughout the hippocampal formation, with densest staining in the main part of the hippocampus, that is, CA1–CA3, and in the hilus of the dentate gyrus. In addition, the proximal third of the molecular layer of the dentate gyrus stained denser than the distal two-thirds. Electron microscopy revealed dense staining of postsynaptic densities apposed to unstained presynaptic terminals in both the stratum oriens and the molecular layers of CA3 and CA1/CA2 regions. This distribution is consistent with evidence that NMDA receptors are postsynaptic in the Schaffer collateral-commissural pathway associated with long-term potentiation in CA1 pyramidal neurons (Kamiya et al., 1993), and that NMDA receptors mediate long-term potentiation in one or more inputs to the CA3 pyramidal neurons, including commissural/associational fiber and/or fimbrial fiber–CA3 systems (Ishihara et al., 1990; Zalutsky and Nicoll, 1990; Katsuki et al., 1991). In contrast, our studies indicate that postsynaptic densities apposed by mossy fiber terminals, which form synapses on the proximal portions (i.e., stratum lucidum) of the apical dendrites of CA3 pyramidal neurons, were usually unstained, although some of these postsynaptic densities possessed light staining. These data are consistent with reports that the long-term potentiation in the mossy fiber–CA3 pyramidal cell synapses is NMDA independent (Zalutsky and Nicoll, 1990; Derrick et al., 1991; Watanabe et al., 1992; see also Weisskopf et al., 1993). Interestingly, Monaghan and Cotman (1985) noted a lack of NMDA-sensitive L-^{3}H-glutamate binding in the stratum lucidum, although we see light microscope evidence of neuropilar staining in this area. Since this staining appears to be concentrated in parallel processes as seen in coronal sections, and we saw staining with electron microscopy in parallel processes that appear to be thin, unmyelinated axons, NMDAR1 may be present in axons of this region, although it is either rare in or absent from the presynaptic terminals of the stratum lucidum. Light microscopic examination of sections of rat brain stained with antibodies to the AMPA receptors GluR2/3 and possibly -4 revealed a similar staining pattern in the stratum lucidum (see Fig. 10*e,f* in Petralia and Wenthold, 1992). In a related study, Martin et al. (1993) described immunostaining for GluR1 in axons of the Schaffer–commissural fiber region of the hippocampus, although no presynaptic terminal staining was seen. As suggested by these authors, we cannot rule out the possibility that such axonal staining reflects the presence of presynaptic receptor molecules that are undetectable by our immunocytochemical techniques. However, this seems unlikely since there is little evidence for presynaptic NMDA receptors in the hippocampus (Forsythe and Clements, 1990; see also discussions in Stone and Burton, 1988; Geddes et al., 1992), with the possible exception of presynaptic NMDA receptors on the varicosities of noradrenergic fibers (Pittaluga and Raiteri, 1990; Wang et al., 1992). The latter were not identified in our study, but it is possible that the stained axons and/or other unidentified, stained processes are noradrenergic, since noradrenergic processes are common in the stratum lucidum of the rat (Loy et al., 1980). Other possibilities are that axonal labeling represents accidental acquisition or functionally different molecules (see discussion in Petralia and Wenthold, 1992). The staining pattern seen in the molecular layer of the dentate gyrus resembles the binding pattern described for NMDA-sensitive L-^{3}H-glutamate binding, with denser staining/binding seen in the proximal third of this layer. Since this region contains the proximal portions of the granule cell dendrites that receive synapses from ipsi- and contralateral hilar cells (see discussions in Amaral, 1987; Brown and Zador, 1990; Geddes et al., 1992), NMDA receptors may play a role in this pathway (Geddes et al., 1992). Presence of some staining in the outer two-thirds of the molecular layer of the dentate gyrus supports a role for NMDA in the perforant path–dentate granule cell synapses of this area (Geddes et al., 1992; Watanabe et al., 1992), although such a role has been contested (discussed in Stone and Burton, 1988).

NMDA receptors in the cerebellar cortex

Immunostaining with antibody to NMDAR1 in the cerebellar cortex was densest in Purkinje cells, moderate in Golgi cells and neuropil of granular and molecular layers, and light in small cells of the molecular layer. With electron microscopy, staining was densest in postsynaptic densities in spines apposed to unstained presynaptic terminals in the molecular layer, and in the cell body and dendrite cytoplasm of Purkinje cells. Most of these synapses appeared to be parallel fiber synapses on Purkinje cell dendritic spines. We did not find definitive evidence of climbing fiber synapses, since it was difficult to corroborate the criteria for these synapses (Mugnaini, 1972; Palay and Chan-Palay, 1974), due to minimal fixation conditions and lack of uranium and lead stains. Some unstained terminals were seen apposed to stained postsynaptic densities on dendritic shafts, suggesting that NMDAR1 may be present at synapses on dendrites of Golgi cells (which can send dendrites into the molecular layer) and/or small cells of the molecular layer.

While many of the stained structures seen in this study of the cerebellar cortex could not be identified with certainty with electron microscopy, due to necessary constraints in the preparation techniques, we are reasonably certain that staining is present in Purkinje cell bodies and dendrites, and postsynaptic densities in Purkinje spines apposed to unstained parallel fibers in the molecular layer. In addition, some evidence was seen of stained postsynaptic densities of small cell dendrites. These data suggest that the NMDAR1 subunit is present in synapses of both Purkinje and small cell dendrites. This correlates with our light microscope findings of staining in Purkinje and Golgi cells and to a lesser extent in small cells of the molecular layer. In addition, *in situ* hybridization has confirmed that RNA for NMDAR1 is present in these cells types (Moriyoshi et al., 1991). The presence of NMDA receptors in synapses of the small inhibitory cells of the rat cerebellum is supported by pharmacological/electrophysiological data (Quinlan and Davies, 1985; Hussain et al., 1991). However, the presence of NMDA receptors on Purkinje cells is disputed (see review in Stone and Burton, 1988). While some studies have supported the presence of these receptors on Purkinje cells (e.g., Quinlan and Davies, 1985; Sekiguchi et al., 1987), other studies have found evidence of the non-NMDA types of glutamate receptors only (e.g., Perkel et al., 1990; Farrant and Cull-Candy, 1991). Audinat et al. (1990) found evidence of NMDA receptors in deep cerebellar nuclei, but not in Purkinje cells, in cerebellar slice cultures. Other studies have indicated that NMDA receptors are present on most Purkinje cells during early postnatal development (Krupa and Crepel, 1990; Rosenmund et al., 1992), but that the number of Purkinje cells with active NMDA receptors becomes reduced with age (Krupa and Crepel, 1990). Such a phenomenon may explain, in part, the variation in density among Purkinje cells as illustrated in our Figure 10*c*, and as we describe in many other structures throughout the brain. The presence of NMDA receptors on Purkinje cells may be masked by interactions with adjacent inhibitory cells that possess more sensitive NMDA receptors (Quinlan and Davies, 1985; review by Stone and Burton, 1988) and/or by the particular sensitivity of these receptors to other factors that affect the functional state of the Purkinje cell (Sekiguchi et al., 1987; Hussain et al., 1991). Note also that, so far, only the presence of NMDAR1 has been demonstrated in Purkinje cells. Current amplitudes obtained in *Xenopus* oocytes with homomeric NMDAR1 complexes are very small (Moriyoshi et al., 1991); that is, the NMDAR1 subunit must combine with NMDAR2 subunits to produce the level of responses seen typically in the brain (review by Nakanishi, 1992). Furthermore, the major form of NMDAR1 in the cerebellum appears to be the R1B isoform, which is less sensitive than R1A (major isoform of the brain) to NMDA and glutamate (N. Nakanishi et al., 1992). Finally, the exact location of the NMDA receptors of Purkinje cells is still not definite, since our data indicate that NMDAR1 may be present at the parallel fiber synapses, but leave open the possibility that NMDA receptors are present at the climbing fiber synapse, as suggested by others (Sekiguchi et al., 1987).

The low level of staining seen with electron microscopy in the granule cell layer is not surprising considering that our light microscope studies revealed only a moderate level of staining in this layer. However, it seems somewhat contrary to binding studies that show high levels in the granule cell layer (Monaghan and Cotman, 1985; Jansen et al., 1990) and electrophysiological studies that indicate that NMDA receptors are present at the mossy fiber–granule cell synapse (Garthwaite and Brodbelt, 1989; D'Angelo et al., 1990; Silver et al., 1992) and that they colocalize with non-NMDA receptors at this synapse (Garthwaite and Brodbelt, 1989; Silver et al., 1992). Possible explanations for the lack of dense staining include the following. (1) There are few active NMDA receptors at this synapse (Silver et al., 1992), that is, not detectable at the antibody concentrations used. (2) NMDAR1 in the granule cell layer may be particularly sensitive to fixation or other preparation artifacts. (3) The NMDA receptors found in the mossy fiber–granule cell synapse are of a type not detected by our antibody; for example, they may be composed of an NMDAR1 isoform not recognized by our antibody (discussed above), along with one or more of the NMDAR2 subunits (Monyer et al., 1992).

NMDA receptors in other regions

In this study, we found evidence of NMDAR1 throughout many structures in the nervous system, as is supported by numerous pharmacological studies (older work reviewed by Stone and Burton, 1988). For example, a number of forebrain structures contained moderate to dense staining in correspondence with pharmacological evidence of active involvement of NMDA receptors in neurotransmission, including cultured olfactory bulb neurons (Trombley and Westbrook, 1990), piriform cortex (long-term potentiation; Kanter and Haberly, 1990), amygdala (Nakanishi et al., 1990), dopaminergic neurons of the substantia nigra (Mereu et al., 1991), vertical limb of the diagonal band (modulation of ACh release; Nishimura and Boegman, 1990), and striatum (Calabresi et al., 1992). In the hypothalamus, our findings of dense immunostaining in certain neurons, notably those of the supraoptic and paraventricular nuclei, support a role for NMDA receptors in the regulation of neurosecretion by neurons of the hypothalamus (Hu and Bourque, 1991; Rage et al., 1991, 1993). In support of our findings, significant staining in the paraventricular nucleus with an antibody to NMDAR1 has been reported in a preliminary study (Fotuhi et al., 1992). The findings of moderate to dense immunostaining with antibody to NMDAR1 in many structures of the brainstem and spinal cord, including many populations of reticular, sensory, and especially motor neurons, are supported by numerous pharmacological/electrophysiological studies, which indicate the presence of NMDA receptors on or associated with many types of brainstem and spinal cord neurons (see review by Stone and Burton, 1988),

including rubrospinal neurons of the red nucleus (Billard et al., 1991); inferior collicular, pontine reticular, and spinal cord neurons associated with auditory startle behavior (Boulis et al., 1990; Ebert and Koch, 1992; Faingold et al., 1992); neurons of the nucleus of the solitary tract associated with swallowing (Kessler and Jean, 1991); Vth motoneurons associated with the jaw-opening reflex (Katakura and Chandler, 1991); neurons associated with various cardiorespiratory reflexes (Greer et al., 1991; Jung et al., 1991; Varner et al., 1992); noradrenergic neurons of the locus coeruleus (Aston-Jones et al., 1991); and possible interneurons associated with spinothalamic tract neurons and hyperalgesia (Dougherty et al., 1992). There is much evidence supporting a role of NMDA receptors in vestibular compensation and other aspects of neural plasticity in the vestibular system (reviews by Darlington et al., 1991; Smith et al., 1991). Many of these studies have concentrated on these phenomena in the medial vestibular nucleus (Capocchi et al., 1992; Serafin et al., 1992; Smith and Darlington, 1992), which also contains significant binding for NMDA receptors (Monaghan and Cotman, 1985). In comparison, our findings have indicated that there are substantial amounts of NMDA receptors in several vestibular nuclei, especially the superior, small nuclei, as well as some neurons of the lateral, and with less in the spinal vestibular nucleus. In contrast, staining in the medial vestibular nucleus was mostly neuropilar, with only low to moderate levels in the neuron cell bodies. This may be due to a distribution of NMDAR1 that is concentrated mainly on certain neuropilar elements, with a relatively lower abundance in the cytoplasmic pool, compared to NMDAR1 on neurons in other nuclei of the vestibular nuclear complex. Alternatively or in addition, this discrepancy could be due to the presence of additional NMDA receptor subtypes or isoforms not recognized by our antibody, as discussed above.

Immunostaining in the thalamus was moderate overall, although certain nuclei showed denser staining of some neurons. Similarly, binding studies revealed considerable variation among different nuclei. Perhaps, most interesting is the correlation of low to moderate expression of NMDA receptors, seen with both immunocytochemistry and binding studies, in structures shown to have NMDA receptors in pharmacological/electrophysiological studies. For example, we found only low to moderate staining overall in the lateral habenula and zona incerta, similar to the rather low amount of binding seen in the habenula and zona incerta (Monaghan and Cotman, 1985; Maragos et al., 1988), although evidence of functional NMDA receptors has been found in both of these structures (De Sarro et al., 1992; H. Nakanishi et al., 1992). This supports the contention that the light to moderate staining that we see in many structures throughout the nervous system is indicative of the presence of active NMDA receptors. Notable also is the reuniens nucleus, which stains moderately overall as do all of the midline thalamic nuclei, but differs from the other nuclei in containing many moderately densely stained neurons. This nucleus appears to contain NMDA receptors that are involved in modulation of temporal limbic excitability, as may relate to epileptic seizures (Hirayasu and Wada, 1992).

Colocalization of NMDA receptors with other glutamate receptor types

This study has shown that the NMDAR1 subunit is present in most nuclei in the CNS, as suggested by the previous *in situ* hybridization study (Moriyoshi et al., 1991). Comparison of our data on distribution of NMDAR1 with those of other glutamate receptor types is facilitated by the publication of several comprehensive surveys on AMPA receptors (*in situ* hybridization, Sato et al., 1993; immunocytochemistry, Petralia and Wenthold, 1992; Martin et al., 1993) as well as one on metabotropic glutamate receptors (*in situ* hybridization, Shigemoto et al., 1992a). Comparison of localization data in our Appendix and Results with those published in these articles, as well as with those of smaller studies (see introductory remarks), reveals many nuclei and neuron types that show high levels of two or more types of glutamate receptors. Rat barrel fields in the primary somatosensory cortex are delineated with immunostaining for NMDAR1 as well as the kainate receptor subunit GluR6 (Petralia, Wang, and Wenthold, unpublished observations), but are not differentially stained with an antibody to the AMPA receptor subunit GluR1 (discussed above). Mitral cells of the main olfactory bulb appear to contain substantial levels of NMDAR1, NMDAR2C (Monyer et al., 1992), GluR1–GluR4, and the metabotropic receptor subunit mGluR1, confirming pharmacological/electrophysiological studies indicating the presence of NMDA, non-NMDA, and possibly metabotropic glutamate receptors associated with mitral cells (Trombley and Westbrook, 1990). CA1 pyramidal cells bear receptors for NMDAR1 and GluR1–GluR4, but may have comparatively little mGluR1, so the exact nature of the involvement of metabotropic glutamate receptors in long-term potentiation (along with NMDA and AMPA receptors) in these cells (Baskys and Malenka, 1991; review by Anwyl, 1991) remains uncertain, and may involve interneurons (Martin et al., 1992). In contrast, CA3 pyramidal cells have substantial amounts of NMDAR1, GluR1–GluR4, and mGluR1, as well as some of the kainate subunits (pyramidal cell layer—GluR6, Egebjerg et al., 1991; KA1, KA2, Herb et al., 1992). This complexity of subtypes reflects the complexity of circuitry; that is, long-term potentiation occurs at two or more different synaptic inputs, of which at least one utilizes NMDA receptors, while another (mossy fiber input) involves non-NMDA and opioid receptors (Ishihara et al., 1990; see discussion above). Cerebellar Purkinje cells have high levels of NMDAR1, GluR2 and -3, and mGluR1. The two major excitatory inputs, that is, parallel and climbing fibers (e.g., Crepel et al., 1982; review by Llinas and Walton, 1990), may express mGluR1 and GluR2/3, respectively, possibly in relation to the development of long-term depression (Martin et al., 1992), but the exact relationships to this circuitry are unclear. However, the role played by NMDA receptors in Purkinje cell circuitry is even less certain (see above). Our results indicated that NMDAR1 may be present at parallel fiber–Purkinje dendritic spine synapses, while localization of this subunit at climbing fiber–Purkinje cell synapses was not determined. A detailed electron microscopic study of localization of different types of glutamate receptors on Purkinje cells is needed to help clarify the relationships. Comparison of the immunocytochemical and *in situ* hybridization data on subtype localization in many other structures of the nervous system reveals frequent colocalization of NMDA and non-NMDA receptors, which is corroborated by pharmacological/electrophysiological studies (review by Collingridge and Lester, 1989), such as for the two main inputs to the superficial layers of the piriform cortex (Jung et al., 1990), dopaminergic neurons of the substantia nigra (Mereu et al., 1991), neurosecretory cells of the supraoptic hypothalamic nucleus (Hu and Bourque, 1991), and rubrospinal neurons of the red nucleus (Billard et al., 1991). However, much still needs to be learned about patterns of co-

localization of different glutamate receptor types on individual neurons and, more importantly, within individual synapses (Bekkers and Stevens, 1989; Jones and Baughman, 1991).

Appendix

Localization of NMDAR1 (AbT3) in the rat brain

Level of staining is based on an arbitrary relative scale from 0 to 4, where 0 represents the level seen in corresponding control sections and 4 is the densest staining.

I. Forebrain	
A. Isocortex	
1. Frontal cortex, area 1	2
2. Frontal cortex, area 2	2
3. Forelimb/hindlimb area	2
4. Temporal cortex, area 1 (prim. aud.)	2
5. Occipital cortex, area 1	2–2.5
6. Medial occipital area 2	2
7. Parietal cortex, area 1	2
I	1.5
II	2
III	2.5
IV	1.5–2
V	2.5
VI	2
VI (deep layer)	2.5
White matter	0–0.5
8. Parietal cortex, area 2	2
B. Allocortex	
1. Cingulate cortex, area 1,2	1.5–2
2. Perirhinal cortex	2.5
3. Insular cortex	2
4. Retrosplenial agranular cortex	2.5
5. Retrosplenial granular cortex	1.5–2
C. Claustrum	2.5
D. Olfactory regions	
1. Anterior olfactory n.	2.5
2. Olfactory tubercle	3
3. Piriform cortex	2.5–3
Layer Ia	2–2.5
Layer Ib	1–1.5
Layer II	2.5–3
Layer III	2
4. Accessory olfactory bulb	
Vomeronasal nerve layer	1.5–2
Processes of glomerular layer	2.5
External plexiform layer (EPL)	2–2.5
Neuron cell bodies in EPL	2.5–3
Internal plexiform layer	0–1
Granule cells	2–2.5
5. Main olfactory bulb	
Olfactory nerve	2.5
Glomeruli	2
Processes of glomerular layer	2.5
Periglomerular cells	2.5
External plexiform layer (EPL)	2–2.5
Neuron cell bodies in EPL	2.5
Mitral cells	3
Internal plexiform layer	1.5–2
Granule cells: superficial	2
Granule cells: deep	2.5
Short axon cells of granule c. layer	1–2
E. Hippocampal formation (cortex)	
1. Entorhinal cortex	2–3
2. Subicular complex	
Parasubiculum	2.5
Presubiculum	2–2.5
Subiculum	2.5
3. CA1	
Molecular layer	2–2.5
Pyramidal layer	3.5
Stratum oriens	2–2.5
4. CA2, CA3	
Molecular layer	
Distal portion	2
Proximal portion (varies with section position)	2–3
Pyramidal layer	4
Stratum oriens	2.5
5. Dentate gyrus	
Molecular layer	
Outer ⅔	1.5
Inner ⅓	2.5
Granular layer	2–2.5
Polymorph layer (hilus)	2.5
Neuropil	2
Neurons	3–4
6. Induseum griseum	2.5–3
7. Tenia tecta	2.5–3
F. Amygdala	
1. Medial n.	1–2
2. Posteromedial cortical n.	2–2.5
3. Lateral n.	1–2
4. Basolateral n.	2.5
5. Basomedial n.	1–2
6. Dorsal endopiriform n.	2–2.5
G. Septum	
1. Lateral nucleus	
Pars dorsalis	2–2.5
Pars ventralis	1.5–2
2. Septohippocampal n.	2.5
H. Basal ganglia	
1. Caudate-putamen	2–3
2. Nucleus accumbens	2–3
3. Globus pallidus	1–1.5
4. Ventral pallidum	2
5. Horizontal limb of the diagonal band	2.5
6. Vertical limb of the diagonal band	2–2.5
7. Subthalamic nucleus	2
8. Substantia nigra	
Compact part	2.5–3
Reticular, lateral parts	2–2.5
I. Epithalamus	
1. Medial habenula	3
2. Lateral habenula	1.5–2.5
3. Pineal gland	2.5–3
J. Thalamus	
1. Ventral nuclear group	
Ventrolateral n.	2–3
Ventromedial n.	2–3
Ventroposterolateral n.	2.5–3
Ventroposteromedial n.	2–3
2. Lateral nuclear group	
Laterodorsal n.	1.5–2
Lateral posterior n.	2
3. Anterior nuclear group	
Anteroventral n.	2–2.5
Anterodorsal n.	2.5
Anteromedial n.	1.5
Interanteromedial n.	1.5
4. Central medial n.	2
5. Midline group	
Rhomboidal n.	2
Anterior paraventricular n.	2–2.5
Reuniens n.	2
6. Reticulothalamic n.	2–2.5
7. Zona incerta	1.5–2.5
8. Lateral geniculate n.	
Dorsolateral n.	2.5
Ventrolateral n.	2
9. Medial geniculate n.	
Dorsal portion	1.5–2
Ventral portion	2
Medial portion	2
Suprageniculate n.	2–2.5
K. Hypothalamus	
1. Supraoptic n.	3–3.5
2. Retrochiasmatic portion of the supraoptic n.	3.5–4
3. Paraventricular n., magnocellular portion	3–3.5

4. Periventricular n.	2
5. Lateral hypothalamic area	1.5–2
6. Posterior n.	2
7. Arcuate n.	2.5–3
8. Medial mammillary n.	2
9. Junction-median eminence/infundibulum	2.5
L. Pituitary gland	
1. Anterior lobe	2.5–3
2. Intermediate lobe	3–3.5
3. Posterior lobe	3
M. Subcommissural organ	2.5
N. White matter	
1. Corpus callosum	0.5–1
2. Internal capsule	0.5–1
3. Optic chiasm	0–0.5
4. Supraoptic decussation	1–1.5
5. Anterior commissure	
Anterior	0–1
Posterior	1–2
6. Posterior commissure	0
7. Medial lemniscus	0–1
II. Brainstem	
A. Sensory	
1. Visual system	
Superior colliculus	
Superficial gray	2.5
Optic nerve layer	1.5–2
Intermediate gray	2
Intermediate white	1.5–2
Deep gray	2
Large multipolar neurons, lateral lay. 3	3–4
Parabigeminal n.	2
2. Vth cranial nerve	
Mesencephalic n. V neurons	3–3.5
Spinal n. V	
Oral part	2
Interpolar part	2–3
Caudal part	
Marginal zone	3
Gelatinous layer	2.5–3
Magnocellular layer	2–2.5
Principal n. V	
Dorsomedial	2.5
Ventrolateral	2
3. Auditory nuclei	
Cochlear nuclei	
Anteroventral	2
Posteroventral	2.5–3
Dorsal, layers 1, 2	3.5
N. trapezoid body	2.5
Superior olive	
Lateral	2.5–3
Medial	2.5–3
Periolivary nuclei	
Superior	2–2.5
Dorsal	2–2.5
Lateroventral	2.5
Medioventral	2.5
N. lateral lemniscus	
Dorsal	2.5
Intermediate	2.5
Ventral	3
Inferior colliculus	
External (rostral part)	2–2.5
Central	1.5–2
Dorsal	2.5
4. Vestibular nuclei	
Medial n.	2.5–3
Lateral n.	
Neuropil	1–2
Neurons	2–3.5
Superior n.	2.5–3
Spinal n.	2
Nucleus X	2.5–3
Nucleus Y	2.5–3
Prepositus hypoglossal n.	2.5–3
5. Solitary n.	2.5
6. Gracile n.	3–3.5
7. Cuneate n.	2.5
8. External cuneate n.	2.5–3.5
B. Motor	
1. Oculomotor n. (III)	3
2. Edinger-Westphal n.	2.5
3. Abducens n. (VI)	3
4. Motor n. V	
Neuropil	2–2.5
Neurons	3.5–4
5. Facial n. (VII)	
Neuropil	2.5
Neurons	3.5
6. Ambiguus n.	3.5
7. Dorsal motor n. vagus (X)	2.5
8. Hypoglossal n. (XII)	3–3.5
9. Large neurons of supraspinal n.	3.5–4
C. Reticular core, including central gray	
1. Pontine nuclei	3
2. Interpeduncular n.	3
3. Red n.	3
Neuropil	1.5–2
Neurons	3–4
4. Inferior olive	3–3.5
5. Reticular formation	
Gigantocellular/paragigantocellular n.	1.5–2
Gigantocellular n., alpha	2
Lateral n.	3.5
Lateral n., parvocellular	3
Pontine n., caudal part	1.5–2
Pontine n., oral part	2
Parvocellular n.	2
6. Raphe n.	
Magnus	1.5–2
Obscurus	1.5–2
Pallidus	2
7. Mesencephalic central gray	2
8. Microcellular tegmental n.	2.5
D. White matter	
1. Dorsal spinocerebellar tract	0.5–1
2. Tract n. V	0–0.5
3. Tract n. VII	0–1
E. Locus coeruleus	3
F. Area postrema	2.5–3
III. Cerebellum	
A. Deep nuclei	
1. Interpositus	2–2.5
2. Lateral	3
3. Medial	2–2.5
B. Cortex	
1. Molecular layer	2–3
2. Granular layer	2–2.5
3. Bergmann glia	0–1
4. Purkinje cell bodies	3.5–4
5. Purkinje cell dendrites	2.5–3
6. Molecular layer cells	1–2
7. Golgi cells	2–3
8. White matter	0–0.5
Glia	1
C. Cerebellar peduncles	
1. Inferior	0-0.5
Glia	1.5
2. Middle	0–0.5
3. Superior	0–0.5
IV. Cervical spinal cord	
A. Laminae I–III	3–3.5
B. Laminae VII–VIII	2
C. Motoneurons of lamina IX	3.5–4
D. Lamina X	2.5–3
V. Ganglia	
A. Vestibular ganglion cells	2–3
B. Cervical dorsal root ganglion cells	3–3.5

References

Amaral DG (1987) Memory: anatomical organization of candidate brain regions. In: Handbook of physiology, Sec 1, The nervous system, Vol V, Higher functions of the brain, Pt 1 (Plum F, ed), pp 211–294. Bethesda, MD: American Physiological Society.

Anwyl R (1991) The role of the metabotropic receptor in synaptic plasticity. Trends Pharmacol Sci 12:324–326.

Armstrong WE (1985) Hypothalamic supraoptic and paraventricular nuclei. In: The rat nervous system, Vol 1 (Paxinos G, ed), pp 119–128. New York: Academic.

Armstrong-James M, Welker E, Callahan CA (1993) The contribution of NMDA and non-NMDA receptors to fast and slow transmission of sensory information in the rat SI barrel cortex. J Neurosci 13:2149–2160.

Aston-Jones G, Shipley MT, Chouvet G, Ennis M, van Bockstaele E, Pieribone V, Shiekhattar R, Akaoka H, Drolet G, Astier B, Charléty P, Valentino RJ, Williams JT (1991) Afferent regulation of locus coeruleus neurons: Anatomy, physiology and pharmacology. In: Progress in brain research (Barnes CD, Pompeiano O, eds), pp 47–75. New York: Elsevier.

Audinat E, Knöpfel T, Gähwiler BH (1990) Responses to excitatory amino acids of Purkinje cells and neurones of the deep nuclei in cerebellar slice cultures. J Physiol (Lond) 430:297–313.

Baskys A, Malenka RC (1991) *Trans*-ACPD depresses synaptic transmission in the hippocampus. Eur J Pharmacol 193:131–132.

Bayer SA (1985) Hippocampal region. In: The rat nervous system, Vol 1 (Paxinos G, ed), pp 335–352. New York: Academic.

Beaton JA, Stemsrud K, Monaghan DT (1992) Identification of a novel *N*-methyl-D-aspartate receptor population in the rat medial thalamus. J Neurochem 59:754–757.

Bekkers JM, Stevens CF (1989) NMDA and non-NMDA receptors are co-localized at individual excitatory synapses in cultured rat hippocampus. Nature 341:230–233.

Bettler B, Boulter J, Hermans-Borgmeyer I, O'Shea-Greenfield A, Deneris ES, Moll C, Borgmeyer U, Hollmann M, Heinemann S (1990) Cloning of a novel glutamate receptor subunit, GluR5: expression in the nervous system during development. Neuron 5:583–595.

Billard JM, Daniel H, Pumain R (1991) Sensitivity of rubrospinal neurons to excitatory amino acids in the rat red nucleus *in vivo*. Neurosci Lett 134:49–52.

Blackstad TW, Kjaerheim A (1961) Special axo-dendritic synapses in the hippocampal cortex: electron and light microscopic studies on the layer of mossy fibers. J Comp Neurol 117:133–159.

Boulis NM, Kehne JH, Miserendino MJD, Davis M (1990) Differential blockade of early and late components of acoustic startle following intrathecal infusion of 6-cyano-7-nitroquinoxaline-2,3-dione (CNQX) or D,L-2-amino-5-phosphonovaleric acid (AP-5). Brain Res 520:240–246.

Boulter J, Hollmann M, O'Shea-Greenfield A, Hartley M, Deneris E, Maron C, Heinemann S (1990) Molecular cloning and functional expression of glutamate receptor subunit genes. Science 249:1033–1037.

Brooks WJ, Petit TL, LeBoutillier JC, Lo R (1991) Rapid alteration of synaptic number and postsynaptic thickening length by NMDA: an electron microscopic study in the occipital cortex of postnatal rats. Synapse 8:41–48.

Brown TH, Zador AM (1990) Hippocampus. In: The synaptic organization of the brain (Shepherd GM, ed), pp 346–388. New York: Oxford UP.

Calabresi P, Maj R, Pisani A, Mercuri NB, Bernardi G (1992) Long-term synaptic depression in the striatum: physiological and pharmacological characterization. J Neurosci 12:4224–4233.

Capocchi G, Torre GD, Grassi S, Pettorossi VE, Zampolini M (1992) NMDA receptor-mediated long term modulation of electrically evoked field potentials in the rat medial vestibular nuclei. Exp Brain Res 90: 546–550.

Carpenter MB, Sutin J (1983) Human neuroanatomy, 8th ed. Baltimore: Williams & Wilkins.

Chazot PL, Cik M, Stephenson FA (1992) Immunological detection of the NMDAR1 glutamate receptor subunit expressed in human embryonic kidney 293 cells and in rat brain. J Neurochem 59:1176–1178.

Chen C, Okayama H (1987) High-efficiency transformation of mammalian cells by plasmid DNA. Mol Cell Biol 7:2745–2752.

Cline HT, Constantine-Paton M (1989) NMDA receptor antagonists disrupt the retinotectal topographic map. Neuron 3:413–426.

Collingridge GL, Lester RAJ (1989) Excitatory amino acid receptors in the vertebrate central nervous system. Pharmacol Rev 41:143–210.

Collingridge GL, Singer W (1990) Excitatory amino acid receptors and synaptic plasticity. Trends Pharmacol Sci 11:290–296.

Cox CL, Metherate R, Weinberger NM, Ashe JH (1992) Synaptic potentials and effects of amino acid antagonists in the auditory cortex. Brain Res Bull 28:401–410.

Crepel F, Dhanjal SS, Sears TA (1982) Effect of glutamate, aspartate and related derivatives on cerebellar Purkinje cell dendrites in the rat: an *in vitro* study. J Physiol (Lond) 329:297–317.

D'Angelo E, Rossi P, Garthwaite J (1990) Dual-component NMDA receptor currents at a single central synapse. Nature 346:467–470.

Darlington CL, Flohr H, Smith PF (1991) Molecular mechanisms of brainstem plasticity. The vestibular compensation model. Mol Neurobiol 5:355–368.

Daw NW, Stein PSG, Fox K (1993) The role of NMDA receptors in information processing. Annu Rev Neurosci 16:207–222.

Derrick BE, Weinberger SB, Martinez JL (1991) Opioid receptors are involved in an NMDA receptor-independent mechanism of LTP induction at hippocampal mossy fiber–CA3 synapses. Brain Res Bull 27:219–223.

De Sarro G, Meldrum BS, De Sarro A, Patel S (1992) Excitatory neurotransmitters in the lateral habenula and pedunculopontine nucleus of rat modulate limbic seizures induced by pilocarpine. Brain Res 591:209–222.

Dougherty PM, Palecek J, Paleckova V, Sorkin LS, Willis WD (1992) The role of NMDA and non-NMDA excitatory amino acid receptors in the excitation of primate spinothalamic tract neurons by mechanical, chemical, thermal, and electrical stimuli. J Neurosci 12:3025–3041.

Durand GM, Gregor P, Zheng X, Bennett MVL, Uhl GR, Zukin RS (1992) Cloning of an apparent splice variant of the rat *N*-methyl-D-aspartate receptor NMDAR1 with altered sensitivity to polyamines and activators of protein kinase C. Proc Natl Acad Sci USA 89:9359–9363.

Ebert U, Koch M (1992) Glutamate receptors mediate acoustic input to the reticular brain stem. Neuroreport 3:429–432.

Egebjerg J, Bettler B, Hermans-Borgmeyer I, Heinemann S (1991) Cloning of a cDNA for a glutamate receptor subunit activated by kainate but not AMPA. Nature 351:745–748.

Faingold CL, Naritoku DK, Copley CA, Randall ME, Riaz A, Boersma Anderson CA, Arneric SP (1992) Glutamate in the inferior colliculus plays a critical role in audiogenic seizure initiation. Epilepsy Res 13: 95–105.

Farrant M, Cull-Candy SG (1991) Excitatory amino acid receptor-channels in Purkinje cells in thin cerebellar slices. Proc R Soc Lond [Biol] 244:179–184.

Fields RD, Yu C, Nelson PG (1991) Calcium, network activity, and the role of NMDA channels in synaptic plasticity *in vitro*. J Neurosci 11:134–146.

Fink K, Bönisch H, Göthert M (1990) Presynaptic NMDA receptors stimulate noradrenaline release in the cerebral cortex. Eur J Pharmacol 185:115–117.

Fink K, Schultheiß R, Göthert M (1992) Stimulation of noradrenaline release in human cerebral cortex mediated by *N*-methyl-D-aspartate (NMDA) and non-NMDA receptors. Br J Pharmacol 106:67–72.

Forsythe ID, Clements JD (1990) Presynaptic glutamate receptors depress excitatory monosynaptic transmission between mouse hippocampal neurones. J Physiol (Lond) 429:1–16.

Fotuhi M, Sharp AH, Snyder SH, Dawson TM (1992) Differential localization of the metabotropic (mGluR1) and NMDA receptors in the brain. Soc Neurosci Abstr 18:1149.

Furuyama T, Kiyama H, Sato K, Park HT, Maeno H, Takagi H, Tohyama M (1993) Region-specific expression of subunits of ionotropic glutamate receptors (AMPA-type, KA-type and NMDA receptors) in the rat spinal cord with special reference to nociception. Mol Brain Res 18:141–151.

Gallo V, Upson LM, Hayes WP, Vyklicky L, Winters CA, Buonanno A (1992) Molecular cloning and developmental analysis of a new glutamate receptor subunit isoform in cerebellum. J Neurosci 12: 1010–1023.

Garthwaite J, Brodbelt AR (1989) Synaptic activation of *N*-methyl-D-aspartate and non-*N*-methyl-D-aspartate receptors in the mossy fibre pathway in adult and immature rat cerebellar slices. Neuroscience 29:401–412.

Geddes JW, Brunner L, Cotman CW, Buzsáki G (1992) Alterations in [^{3}H]kainate and *N*-methyl-D-aspartate-sensitive L-[^{3}H]-glutamate

binding in the rat hippocampal formation following fimbria-fornix lesions. Exp Neurol 115:271–281.
Greer JJ, Smith JC, Feldman JL (1991) Role of excitatory amino acids in the generation and transmission of respiratory drive in neonatal rat. J Physiol (Lond) 437:727–749.
Hennegriff M, Bahr BA, Hail RA, Guthrie KM, Yamamoto RS, Kessler M, Gall CM, Lynch G (1992) Antibodies to the GluR-A, GluR-B/C, GluR-D, and NMDA-R1 glutamate receptor subunits: Western blot studies. Soc Neurosci Abstr 18:88.
Herb A, Burnashev N, Werner P, Sakmann B, Wisden W, Seeburg PH (1992) The KA-2 subunit of excitatory amino acid receptors shows widespread expression in brain and forms ion channels with distantly related subunits. Neuron 8:775–785.
Hirayasu Y, Wada JA (1992) *N*-methyl-D-aspartate injection into the massa intermedia facilitates development of limbic kindling in rats. Epilepsia 33:965–970.
Hollmann M, O'Shea-Greenfield A, Rogers SW, Heinemann S (1989) Cloning by functional expression of a member of the glutamate receptor family. Nature 342:643–648.
Houamed KM, Kuijper JL, Gilbert TL, Haldeman BA, O'Hara PJ, Mulvihill ER, Almers W, Hagen FS (1991) Cloning, expression, and gene structure of a G protein–coupled glutamate receptor from rat brain. Science 252:1318–1321.
Hu B, Bourque CW (1991) Functional *N*-methyl-D-aspartate and non-*N*-methyl-D-aspartate receptors are expressed by rat supraoptic neurosecretory cells *in vitro*. J Neuroendocrinol 3:509–514.
Hussain S, Gardner CR, Bagust J, Walker RJ (1991) Receptor subtypes involved in responses of Purkinje cell to exogenous excitatory amino acids and local electrical stimulation in cerebellar slices in the rat. Neuropharmacology 30:1029–1037.
Ikeda K, Nagasawa M, Mori H, Araki K, Sakimura K, Watanabe M, Inouc Y, Mishina M (1992) Cloning and expression of the ε4 subunit of the NMDA receptor channel. FEBS Lett 313:34–38.
Ishihara K, Katsuki H, Sugimura M, Kaneko S, Satoh M (1990) Different drug-susceptibilities of long-term potentiation in three input systems to the CA3 region of the guinea pig hippocampus *in vitro*. Neuropharmacology 29:487–492.
Ishizuka N, Weber J, Amaral DG (1990) Organization of intrahippocampal projections originating from CA3 pyramidal cells in the rat. J Comp Neurol 295:580–623.
Izquierdo I (1991) Role of NMDA receptors in memory. Trends Pharmacol Sci 12:128–129.
Izumi Y, Clifford DB, Zorumski CF (1992) Inhibition of long-term potentiation by NMDA-mediated nitric oxide release. Science 257: 1273–1276.
Jaarsma D, Sebens JB, Korf J (1991) Localization of NMDA and AMPA receptors in rat barrel field. Neurosci Lett 133:233–236.
Jansen KLR, Faull RLM, Dragunow M, Waldvogel H (1990) Autoradiographic localisation of NMDA, quisqualate and kainic acid receptors in human spinal cord. Neurosci Lett 108:53–57.
Jones KA, Baughman RW (1991) Both NMDA and non-NMDA subtypes of glutamate receptors are concentrated at synapses on cerebral cortical neurons in culture. Neuron 7:593–603.
Jung MW, Larson J, Lynch G (1990) Role of NMDA and non-NMDA receptors in synaptic transmission in rat piriform cortex. Exp Brain Res 82:451–455.
Jung R, Bruce EN, Katona PG (1991) Cardiorespiratory responses to glutamatergic antagonists in the caudal ventrolateral medulla of rats. Brain Res 564:286–295.
Kamiya H, Sawada S, Yamamoto C (1993) Long-lasting potentiation of synaptic transmission in the Schaffer collateral–commissural pathway of the guinea pig hippocampus by activation of postsynaptic *N*-methyl-D-aspartate receptor. Synapse 13:186–194.
Kanter ED, Haberly LB (1990) NMDA-dependent induction of long-term potentiation in afferent and association fiber systems of piriform cortex *in vitro*. Brain Res 525:175–179.
Karp SJ, Masu M, Eki T, Ozawa K, Nakanishi S (1993) Molecular cloning and chromosomal localization of the key subunit of the human *N*-methyl-D-aspartate receptor. J Biol Chem 268:3728–3733.
Katakura N, Chandler SH (1991) Iontophoretic analysis of the pharmacologic mechanisms responsible for initiation and modulation of trigeminal motoneuronal discharge evoked by intra-oral afferent stimulation. Brain Res 549:66–77.
Kato N (1993) Dependence of long-term depression on postsynaptic metabotropic glutamate receptors in visual cortex. Proc Natl Acad Sci USA 90:3650–3654.
Katsuki H, Kaneko S, Tajima A, Satoh M (1991) Separate mechanisms of long-term potentiation in two input systems to CA3 pyramidal neurons of rat hippocampal slices as revealed by the whole-cell patch-clamp technique. Neurosci Res 12:393–402.
Keinänen K, Wisden W, Sommer B, Werner P, Herb A, Verdoorn TA, Sakmann B, Seeburg PH (1990) A family of AMPA-selective glutamate receptors. Science 249:556–560.
Kessler J-P, Jean A (1991) Evidence that activation of *N*-methyl-D-aspartate (NMDA) and non-NMDA receptors within the nucleus tractus solitarii triggers swallowing. Eur J Pharmacol 201:59–67.
Kito S, Miyoshi R, Nomoto T (1990) Influence of age on NMDA receptor complex in rat brain studied by *in vitro* autoradiography. J Histochem Cytochem 38:1725–1731.
Komuro H, Rakic P (1993) Modulation of neuronal migration by NMDA receptors. Science 260:95–97.
Krupa M, Crepel F (1990) Transient sensitivity of rat cerebellar Purkinje cells to *N*-methyl-D-aspartate during development. A voltage clamp study in *in vitro* slices. Eur J Neurosci 2:312–316.
Kumar KN, Tilakaratne N, Johnson PS, Allen AE, Michaelis EK (1991) Cloning of cDNA for the glutamate-binding subunit of an NMDA receptor complex. Nature 354:70–73.
Kutsuwada T, Kashiwabuchi N, Mori H, Sakimura K, Kushiya E, Araki K, Meguro H, Masaki H, Kumanishi T, Arakawa M, Mishina M (1992) Molecular diversity of the NMDA receptor channel. Nature 358:36–41.
Laemmli UK (1970) Cleavage of structural proteins during the assembly of the head of bacteriophage T4. Nature 227:680–685.
Llinas RR, Walton KD (1990) Cerebellum. In: The synaptic organization of the brain (Shepherd GM, ed), pp 214–245. New York: Oxford UP.
Loy R, Koziell DA, Lindsey JD, Moore RY (1980) Noradrenergic innervation of the adult rat hippocampal formation. J Comp Neurol 189:699–710.
Malenka RC (1991) Postsynaptic events mediating LTP. In: Excitatory amino acids and synaptic transmission (Wheal HV, Thomson AM, eds), pp 303–314. New York: Academic.
Maragos WF, Penney JB, Young AB (1988) Anatomic correlation of NMDA and ^{3}H-TCP-labeled receptors in rat brain. J Neurosci 8:493–501.
Martin LJ, Blackstone CD, Huganir RL, Price DL (1992) Cellular localization of a metabotropic glutamate receptor in rat brain. Neuron 9:259–270.
Martin LJ, Blackstone CD, Levey AI, Huganir RL, Price DL (1993) AMPA glutamate receptor subunits are differentially distributed In rat brain. Neuroscience 53:327–358.
Masu M, Tanabe Y, Tsuchida K, Shigemoto R, Nakanishi S (1991) Sequence and expression of a metabotropic glutamate receptor. Nature 349:760–765.
Meguro H, Mori H, Araki K, Kushiya E, Kutsuwada T, Yamazaki M, Kumanishi T, Arakawa M, Sakimura K, Mishina M (1992) Functional characterization of a heteromeric NMDA receptor channel expressed from cloned cDNAs. Nature 357:70–74.
Mereu G, Costa E, Armstrong DM, Vicini S (1991) Glutamate receptor subtypes mediate excitatory synaptic currents of dopamine neurons in midbrain slices. J Neurosci 11:1359–1366.
Molnár E, Baude A, Richmond SA, Patel PB, Somogyi P, McIlhinney RAJ (1993) Biochemical and immunocytochemical characterization of antipeptide antibodies to a cloned GluR1 glutamate receptor subunit: cellular and subcellular distribution in the rat forebrain. Neuroscience 53:307–326.
Monaghan DT (1991) Agonist- and antagonist-preferring *N*-methyl-D-aspartate receptors and independent activation of their ion channels. In: Excitatory amino acids (Meldrum BS, Moroni F, Simon RP, Woods JH, eds), pp 203–211. New York: Raven.
Monaghan DT, Cotman CW (1985) Distribution of *N*-methyl-D-aspartate-sensitive L-[^{3}H]glutamate-binding sites in rat brain. J Neurosci 5:2909–2919.
Monaghan DT, Bridges RJ, Cotman CW (1989) The excitatory amino acid receptors: their classes, pharmacology, and distinct properties in the function of the central nervous system. Annu Rev Pharmacol Toxicol 29:365–402.
Monyer H, Sprengel R, Schoepfer R, Herb A, Higuchi M, Lomeli H, Burnashev N, Sakmann B, Seeburg PH (1992) Heteromeric NMDA receptors: molecular and functional distinction of subtypes. Science 256:1217–1221.
Moriyoshi K, Masu M, Ishii T, Shigemoto R, Mizuno N, Nakanishi S (1991) Molecular cloning and characterization of the rat NMDA receptor. Nature 354:31–37.

Mugnaini E (1972) The histology and cytology of the cerebellar cortex. In: The comparative anatomy and histology of the cerebellum: the human cerebellum, cerebellar connections, and cerebellar cortex (Larsell O, Jansen J, eds), pp 201–251. Minneapolis: University of Minnesota.

Nakanishi H, Ukai K, Nakagawa T, Watanabe S, Kamata O, Yamamoto K (1990) Enhancement of NMDA receptor-mediated synaptic potential evoked in rat medial-amygdala neuron following olfactory bulbectomy. Brain Res 532:69–75.

Nakanishi H, Yamamoto K, Kita H (1992) Lateral hypothalamus and local stimulation induced postsynaptic responses in zona incerta neurons in an *in vitro* slice preparation of the rat. Brain Res 583:287–291.

Nakanishi N, Axel R, Shenider NA (1992) Alternative splicing generates functionally distinct *N*-methyl-D-aspartate receptors. Proc Natl Acad Sci USA 89:8552–8556.

Nakanishi S (1992) Molecular diversity of glutamate receptors and implications for brain function. Science 258:597–603.

Nishimura LM, Boegman RJ (1990) *N*-methyl-D-aspartate-evoked release of acetylcholine from the medial septum/diagonal band of rat brain. Neurosci Lett 115:259–264.

Palay SL, Chan-Palay V (1974) Cerebellar cortex: cytology and organization. New York: Springer.

Paxinos G, Watson C (1986) The rat brain in stereotaxic coordinates, 2d ed. New York: Academic.

Perkel DJ, Hestrin S, Sah P, Nicoll RA (1990) Excitatory synaptic currents in Purkinje cells. Proc R Soc Lond [Biol] 241:116–121.

Peters A, Palay SL, Webster HF (1991) The fine structure of the nervous system, 3d ed. New York: Oxford UP.

Petralia RS, Wenthold RJ (1992) Light and electron immunocytochemical localization of AMPA-selective glutamate receptors in the rat brain. J Comp Neurol 318:329–354.

Pin J-P, Waeber C, Prezeau L, Bockaert J, Heinemann SF (1992) Alternative splicing generates metabotropic glutamate receptors inducing different patterns of calcium release in *Xenopus* oocytes. Proc Natl Acad Sci USA 89:10331–10335.

Pittaluga A, Raiteri M (1990) Release-enhancing glycine-dependent presynaptic NMDA receptors exist on noradrenergic terminals of hippocampus. Eur J Pharmacol 191:231–234.

Puckett C, Gomez CM, Korenberg JR, Tung H, Meier TJ, Chen XN, Hood L (1991) Molecular cloning and chromosomal localization of one of the human glutamate receptor genes. Proc Natl Acad Sci USA 88:7557–7561.

Quinlan JE, Davies J (1985) Excitatory and inhibitory responses of Purkinje cells, in the rat cerebellum *in vivo*, induced by excitatory amino acids. Neurosci Lett 60:39–46.

Rage F, Pin J-P, Tapia-Arancibia L (1991) Phospholipase A_2 and somatostatin release are activated in response to *N*-methyl-D-aspartate receptor stimulation in hypothalamic neurons in primary culture. J Neuroendocrinol 3:515–522.

Rage F, Alonso G, Tapia-Arancibia L (1993) Stimulatory effect of *N*-methyl-D-aspartate on somatostatin gene expression in cultured hypothalamic neurons. Mol Brain Res 17:287–294.

Rosenmund C, Legendre P, Westbrook GL (1992) Expression of NMDA channels on cerebellar Purkinje cells acutely dissociated from newborn rats. J Neurophysiol 68:1901–1905.

Sakurai SY, Penney JB, Young AB (1993) Regionally distinct *N*-methyl-D-aspartate receptors distinguished by quantitative autoradiography of [^{3}H] MK-801 binding in rat brain. J Neurochem 60:1344–1353.

Sato K, Kiyama H, Tohyama M (1993) The differential expression patterns of messenger RNAs encoding non-*N*-methyl-D-aspartate glutamate receptor subunits (GluR1–4) in the rat brain. Neuroscience 52:515–539.

Sekiguchi M, Okamoto K, Sakai Y (1987) NMDA-receptors on Purkinje cell dendrites in guinea pig cerebellar slices. Brain Res 437:402–406.

Serafin M, Khateb A, de Waele C, Vidal PP, Mühlethaler M (1992) Medial vestibular nucleus in the guinea-pig: NMDA-induced oscillations. Exp Brain Res 88:187–192.

Shigemoto R, Nakanishi S, Mizuno N (1992a) Distribution of the mRNA for a metabotropic glutamate receptor (mGLUR1) in the central nervous system: an *in situ* hybridization study in adult and developing rat. J Comp Neurol 322:121–135.

Shigemoto R, Ohishi H, Nakanishi S, Mizuno N (1992b) Expression of the mRNA for the rat NMDA receptor (NMDAR1) in the sensory and autonomic ganglion neurons. Neurosci Lett 144:229–232.

Silver RA, Traynelis SF, Cull-Candy SG (1992) Rapid-time-course miniature and evoked excitatory currents at cerebellar synapses *in situ*. Nature 355:163–166.

Smith PF, Darlington CL (1992) Comparison of the effects of NMDA antagonists on medial vestibular nucleus neurons in brainstem slices from labyrinthine-intact and chronically labyrinthectomized guinea pigs. Brain Res 590:345–349.

Smith PF, de Waele C, Vidal P-P, Darlington CL (1991) Excitatory amino acid receptors in normal and abnormal vestibular function. Mol Neurobiol 5:369–387.

Sommer B, Seeburg PH (1992) Glutamate receptor channels: novel properties and new clones. Trends Pharmacol Sci 13:291–296.

Stone TW, Burton NR (1988) NMDA receptors and ligands in the vertebrate CNS. Prog Neurobiol 30:333–368.

Subramaniam S, McGonigle P (1991) Quantitative autoradiographic characterization of the binding of (+)-5-methyl-10,11-dihydro-5H-dibenzo[a,d]cyclohepten-5,10-imine ([^{3}H] MK-801) in rat brain: regional effects of polyamines. J Pharmacol Exp Ther 256:811–819.

Sugihara H, Moriyoshi K, Ishii T, Masu M, Nakanishi S (1992) Structures and properties of seven isoforms of the NMDA receptor generated by alternative splicing. Biochem Biophys Res Commun 185:826–832.

Tokunaga A, Otani K (1976) Dendritic patterns of neurons in the rat superior colliculus. Exp Neurol 52:189–205.

Towbin H, Staehelin T, Gordon J (1979) Electrophoretic transfer of proteins from polyacrylamide gels to nitrocellulose sheets: procedure and some applications. Proc Natl Acad Sci USA 76:4350–4354.

Tracey DJ (1985) Somatosensory system. In: The rat nervous system, Vol 2 (Paxinos G, ed), pp 129–152. New York: Academic.

Trombley PQ, Westbrook GL (1990) Excitatory synaptic transmission in cultures of rat olfactory bulb. J Neurophysiol 64:598–606.

Varner KJ, Rutherford DS, Vasquez EC, Brody MJ (1992) Identification of cardiovascular neurons in the rostral ventromedial medulla in anesthetized rats. Hypertension [Suppl II] 19:193–197.

Wang JKT, Andrews H, Thukral V (1992) Presynaptic glutamate receptors regulate noradrenaline release from isolated nerve terminals. J Neurochem 58:204–211.

Watanabe Y, Saito H, Abe K (1992) Effects of glycine and structurally related amino acids on generation of long-term potentiation in rat hippocampal slices. Eur J Pharmacol 223:179–184.

Weisskopf MG, Zalutsky RA, Nicoll RA (1993) The opioid peptide dynorphin mediates heterosynaptic depression of hippocampal mossy fibre synapses and modulates long-term potentiation. Nature 362:423–427.

Welker C, Woolsey TA (1974) Structure of layer IV in the somatosensory neocortex of the rat: description and comparison with the mouse. J Comp Neurol 158:437–454.

Wenthold RJ, Yokotani N, Doi K, Wada K (1992) Immunochemical characterization of the non-NMDA glutamate receptor using subunit-specific antibodies: evidence for a hetero-oligomeric structure in rat brain. J Biol Chem 267:501–507.

Wenthold RJ, Trumpy VA, Zhu WS, Petralia RS (in press) Biochemical and assembly properties of GluR6 and KA2, two members of the kainate receptor family, determined with subunit-specific antibodies. J Biol Chem, in press.

Werner P, Voigt M, Keinänen K, Wisden W, Seeburg PH (1991) Cloning of a putative high-affinity kainate receptor expressed predominantly in hippocampal CA3 cells. Nature 351:742–744.

Yamazaki M, Mori H, Araki K, Mori KJ, Mishina M (1992a) Cloning, expression and modulation of a mouse NMDA receptor subunit. FEBS Lett 300:39–45.

Yamazaki M, Araki K, Shibata A, Mishina M (1992b) Molecular cloning of cDNA encoding a novel member of the mouse glutamate receptor channel family. Biochem Biophys Res Commun 183:886–892.

Zalutsky RA, Nicoll RA (1990) Comparison of two forms of long-term potentiation in single hippocampal neurons. Science 248:1619–1624.

Zheng F, Gallagher JP (1992) Metabotropic glutamate receptors are required for the induction of long-term potentiation. Neuron 9:163–172.